Remote Sensing of Environment 334 (2026) 115201

Contents lists available at ScienceDirect

Remote Sensing of Environment

journal homepage: www.elsevier.com/locate/rse

Delta-X: An airborne remote sensing framework to calibrate hydrodynamic and ecogeomorphic processes responsible for land building in coastal deltas

Marc Simard [a,*], Cathleen E. Jones [a], Robert R. Twilley [b], Edward Castañeda-Moya [c,1], Sergio Fagherazzi [d], Cédric G. Fichot [d], Michael P. Lamb [e], Paola Passalacqua [f,g], Tamlin M. Pavelsky [h], David R. Thompson [a], Saoussen Belhadj-aissa [a], Pradipta Biswas [b], Alexandra Christensen [a], Luca Cortese [d,2], Michael Denbina [a], Carmine Donatelli [d,3], Sarah Flores [a], Andy Fontenot [b,4], Joshua P. Harringmeyer [d], Daniel Jensen [a], John Mallard [f], Justin Nghiem [e], Talib Oliver-Cabrera [a], Ali Reza Payandeh [a], Andre S. Rovai [b,5], Elena Solohin [c], Antoine Soloy [a,6], Bhuvan Varugu [a,7], Dongchen Wang [e], Kyle Wright [g], Xiaohe Zhang [d], Yang Zheng [a]

[a] Jet Propulsion Laboratory, California Institute of Technology, Pasadena, CA, USA
[b] Department of Oceanography and Coastal Sciences, Louisiana State University, Baton Rouge, LA, USA
[c] Institute of Environment, Florida International University, Miami, FL, USA
[d] Department of Earth and Environment, Boston University, Boston, MA, USA
[e] Division of Geological and Planetary Sciences, California Institute of Technology, Pasadena, CA, USA
[f] Fariborz Maseeh Department of Civil, Architectural and Environmental Engineering, The University of Texas at Austin, Austin, TX, USA.
[g] Department of Earth and Planetary Sciences, The University of Texas at Austin, Austin, TX, USA.
[h] Department of Earth, Marine and Environmental Sciences, University of North Carolina, Chapel Hill, NC, USA.

ARTICLE INFO

Edited by Menghua Wang

Keywords:
Delta-X
Mississippi River Delta
Coastal resiliency
Deltaic land sustainability
Marsh elevation
Organic productivity
Sediment transport
Airborne remote sensing

ABSTRACT

Coastal river deltas are highly dynamic regions with hydrological processes that vary on hourly, daily, and seasonal timescales. Soil formation in deltas relies on the balance between mineral sediment deposition, erosion, and organic matter production, which are intricately controlled by vegetation and hydrodynamic conditions. The spatial complexity and rapid variations in flow, particularly due to tides, present a major challenge to spaceborne remote sensing achieving the required spatial resolution and temporal sampling. Here, we present an airborne remote sensing and in situ framework that measures parameters that are critical to calibrate and validate hydrodynamic, sediment transport, morphodynamic, and ecogeomorphic models. We discuss the measurements and models within the context of the NASA Earth Venture-Suborbital Delta-X mission, which implemented the framework in two deltaic regions of the Mississippi River Delta with contrasting hydrological regimes, namely the Atchafalaya (i.e., active, river-dominated) and Terrebonne (inactive, river-abandoned) basins that are undergoing land gain and land loss, respectively. The Delta-X framework uses two airborne radar instruments to monitor hydrodynamic processes, measuring water surface level and slope within channels, and tide-induced water level change within wetlands. In addition, an airborne imaging spectrometer provides estimates of suspended sediment concentrations in open water as well as vegetation type and aboveground biomass. We also discuss how the data are used to calibrate and validate the models that estimate sediment deposition and organic soil production, which build land to offset subsidence and sea level rise.

* Corresponding author.
E-mail address: marc.simard@jpl.nasa.gov (M. Simard).
[1] Miami-Dade County Department of Regulatory and Economic Resources, Division of Environmental Resources Management (DERM), Miami, FL, USA
[2] Department of Earth and Environmental Sciences, Boston College, Chestnut Hill, MA, USA
[3] Atmospheric and Environmental Research, Inc., Lexington, MA, USA.
[4] Coastal Design & Infrastructure Division, GIS Engineering, LLC, Baton Rouge, LA, USA
[5] Smithsonian Environmental Research Center, Edgewater, MD, USA
[6] Edeniq, Inc., Visalia, CA, USA
[7] California Dept. of Water Resources, Sacramento, CA, USA

https://doi.org/10.1016/j.rse.2025.115201
Received 4 March 2025; Received in revised form 30 August 2025; Accepted 12 December 2025
Available online 26 December 2025

1. Introduction

River deltas are geologically young landforms that evolve naturally through a delicate balance between elevation gain from soil accretion and elevation loss from subsidence and erosion, all within an environment subject to highly dynamic water and sediment flux from both the river and the sea [Galloway, 1975; Masselink et al., 2014]. For most river deltas, this balance has been upset by human contributions to sea level rise (SLR) [Passeri et al., 2015], subsidence [Karegar et al., 2017; Nicholls et al., 2021], and sediment starvation [Vasilopoulos et al., 2021; Edmonds et al., 2023], all of which have occurred on very short timescales relative to the geological timescale of delta evolution. Today many of the world's river deltas are experiencing increasing levels of submergence and land loss with reduced natural mechanisms to restore the balance [Syvitski et al., 2009; Syvitski et al., 2022]. Although much has been done to document and quantify the factors contributing to land loss, significantly less is known about organic soil production (i.e., root bio- and necromass productivity) and sediment capture and how they relate to the channel network geometry [Paola et al., 2011; Cortese et al., 2024], which are the very processes that can restore balance.

Most large- and medium-sized deltas worldwide are predicted to drown, as expected exogenous sediment supply is not sufficient to maintain the entire deltaic floodplain under projected relative sea-level rise (RSLR, defined as eustatic SLR plus local subsidence) [Giosan et al., 2014; Syvitski et al., 2022]. Recently, numerous studies have evaluated the probability of local land submergence for a range of SLR scenarios based on updated subsidence measurements from synthetic aperture radar (SAR) interferometry (InSAR), the Global Position System (GPS), lidar, tide gauges, and/or in situ measurements [e.g., Keogh and Törnqvist, 2019; Tang et al., 2021; Wu et al., 2022; Ohenhen et al., 2023; K. Wang et al., 2024] but few account explicitly for local organic soil production, which can be a significant contributor to soil accretion and elevation gain in deltas [Deverel et al., 2020; Keogh et al., 2021]. Better models are needed given the potential human and economic impact of land loss in river deltas and other low-lying areas [Neumann et al., 2015; Jevrejeva et al., 2016; Kulp and Strauss, 2019; Hauer et al., 2020]. The scientific literature contains numerous calls to address this gap with spatially comprehensive measurements of hydrologic and ecogeomorphic controls to build accurate quantitative models [Paola et al., 2011; Giosan et al., 2014; Temmerman and Kirwan, 2015; Fagherazzi et al., 2020; Khojasteh et al., 2021; Nienhuis et al., 2023].

The processes controlling soil accretion depend on interdependent conditions of hydrology, ecology, geomorphology, and climate. Deltas are made of distinct but connected landscape components, such as channels and islands, and the subaerial land is often delineated into distinct hydrogeomorphic zones, which are defined by topography as supratidal, intertidal, or subtidal layers [Bevington et al., 2022], and which have characteristic vegetation types and structures. The spatial scales of landscape heterogeneity vary substantially with vegetation type and river discharge contributions. Contiguous areas with similar ecogeomorphic characteristics of elevation and vegetation cover—which we call "ecogeomorphic cells"—are the building blocks of river deltas and set the spatial scale at which soil accretion processes operate [Simard et al., 2022; Twilley et al., 2019a, 2019b]. Within an ecogeomorphic cell, the vegetation type and structure influence hydrological connectivity and sediment accretion rates [Hiatt and Passalacqua, 2015; Wright et al., 2018]. The dominant processes of trapping and producing sediment are likely to vary between cells due to differences in vegetation type and hydrologic connectivity with nearby channels. To accurately model the spatial variability in delta evolution and its response to external forces at the mesoscale, we need to understand accretion processes at the spatial scale of the ecogeomorphic cells and across the three key timescales of tidal cycle, seasonal river flooding, and vegetation growth period, which are the reoccurring cycles that drive deltaic hydrodynamics. Additionally, understanding the cumulative impact of episodic events such as cold fronts, storms, hurricanes, and their associated flooding is essential for quantifying their influence on delta morphology given their high frequency [Payandeh et al., 2019].

Remote sensing can help efficiently monitor river deltas worldwide and has been used to observe sediment concentrations in water [Nechad et al., 2010; Long and Pavelsky, 2013; Shahzad et al., 2018; Jiang et al., 2021; Salter et al., 2022]; flows across wetlands [Lu and Kwoun, 2008; Oliver-Cabrera and Wdowinski, 2016; Liao et al., 2020; Donatelli et al., 2023a]; ecological processes such as phenology [Byrd et al., 2014; Dronova et al., 2021]; and the impact of and recovery from natural and anthropogenic disturbances [Carle et al., 2015; Rangoonwala et al., 2016; Marlier et al., 2022]. However, the observation repeat interval for many of the spaceborne instruments capable of resolving the ecogeomorphic cells is weeks to months, complicating the study of high frequency processes such as tides. In the absence of rapid revisit or geostationary satellites, only airborne measurements can resolve fast processes such as tidal flow within channels and wetlands. Airborne remote sensing enables acquisition of multiple observations within a short timespan to measure high-frequency processes such as tidal propagation across landscapes. In addition, multiple airborne sensors can collect near-simultaneous measurements of interrelated processes, which is critical to understanding the interplay among organic productivity, hydrodynamics, and sediment transport that leads to delta land loss or gain.

We introduce the Delta-X framework, an airborne remote sensing methodology to calibrate and validate ecogeomorphic and hydrodynamic models of coastal river deltas that account for soil accretion at the spatial and temporal scales at which the processes vary. The framework was implemented in a NASA Earth Venture Suborbital-3 (EVS-3) mission that studied two adjacent regions within the Mississippi River Delta with contrasting hydrological regimes, namely the Atchafalaya (i.e., active, river-dominated) and Terrebonne (i.e., inactive, river-abandoned) basins that are undergoing aggradation (land gain) and erosion (land loss), respectively. In the sections below, the airborne observations, in situ measurements, derived products, and models developed through the Delta-X mission are described as a practical example of implementing the framework. Section 2 lays out the problem to be solved, Section 3 provides a description of the Delta-X framework, which can be applied to any river delta, Section 4 discusses its implementation specifically for the Delta-X mission, Section 5 discusses the models' calibration and validation, and Section 6 summarizes and concludes the paper.

2. Delta-X goals and objectives

The Delta-X science goal is to advance understanding of the fundamental connections between coastal hydrology, ecology, and geomorphology that control various stages of the delta cycle (e.g., river and tidal connectivity, soil elevation gradients) by quantifying the mesoscale patterns—the scale of ecogeomorphic cells—of soil accretion within deltas with sufficient fidelity to identify which parts of a delta can survive under projected RSLR (Fig. 1). The Delta-X framework provides a detailed methodology for implementing a comprehensive study incorporating remote sensing and in situ data to calibrate and validate models that can be used to predict which parts of a specific delta can survive RLSR in the coming decades and centuries. The framework presented here is sufficiently general that it can be applied to deltas worldwide under the influence of natural and anthropogenic drivers. During the Delta-X mission, both active (i.e., Atchafalaya) and inactive (i.e. Terrebonne) coastal deltaic floodplains and associated emergent wetlands were studied.

The combined rate of soil accretion from trapping of external mineral sediment on the one hand and local organic accretion (P, from plant growth) on the other (Fig. 2) determines whether river deltas will retain emergent land. The equation governing the rate of land-surface elevation change, $\partial z/\partial t$, is obtained through mass balance [Paola and Voller, 2005] as

$$\frac{\partial z}{\partial t} = P - \frac{1}{\phi_s}\left(\frac{\partial}{\partial t}(ch) + \vec{\nabla} \bullet \vec{q_s}\right), \quad (1)$$

where c is the depth-averaged volumetric sediment concentration, h is the water depth, $\vec{q_s}$ is the volumetric depth-averaged sediment flux per unit width, and ϕ_s is the volume fraction of solids, a factor that accounts for porosity of the sediment layer.

Vegetation contributes to soil accretion rates directly through organic matter production, P, both above ground (litter) and below ground (roots). Vegetation also contributes indirectly to positive accretion by slowing flow, thereby promoting capture of sediments and limiting their re-entrainment [Leonard and Reed, 2002; Zhang et al., 2024]. However, at the mesoscale, vegetation can reduce hydrological connectivity by increasing friction, resulting in more water and sediment retained in or near the channel network, rather than promoting over-flowing onto islands or nourishing the island interior [Nardin and Edmonds, 2014; Hiatt and Passalacqua, 2017; Hiatt et al., 2018]. The latter effects decrease sediment deposition rates, potentially to the point where some areas may become sediment starved. The overall effect of vegetation is not well constrained, and Delta-X mission was designed to test whether vegetation productivity is critical to sustainability. If so, deltaic areas without vegetation will ultimately drown.

However, vegetation alone might not be enough to sustain all or part of a delta. A dense distributary water-channel network might be required, and the three-dimensional geometry of the channels may be important for delivering sediment across an island at flow rates commensurate with sediment capture. In addition, water must reach the island interior either through overbank flow or through small, possibly intermittent channels extending into the island interior [Salter and Lamb, 2022; Varugu et al., 2025]. A site's proximity to a distributary channel determines whether and how far sediment of a given size and for a given flood stage can be transported with water (advected) across the island and settle out, contributing to soil accretion (Fig. 2). The advection length, L_a, is the horizontal distance that a particle travels before settling [Ganti et al., 2014]. If L_a is small compared to the island size, then that sediment may not reach the island interior. Alternatively, if L_a is large compared to the island size, then much of the sediment will bypass the wetland and be lost to the ocean. The density of the channel network determines island sizes, whereas the advection length is set by sediment settling rate, water velocity, and depth. Delta-X can test whether channelization significantly contributes to sediment supply, capture, and retention to determine the relative importance of the channel network and plant productivity (P) to soil accretion at the sub-island scale.

Plant aboveground biomass and structure (e.g., stem diameter, density, and height) can impact flow velocity through friction and therefore affect the advection length. Because advection length is expected to vary greatly with vegetation type (marshes, mangroves, cypress, pine, etc.), this requires modeling areas containing islands with different size, vegetation types, and densities of channel network. Furthermore, the discharge is seasonal, hence so are advection and channel connectivity. Taken in combination, these natural spatial and temporal variations mean the Delta-X measurements must be made in high and low-productivity seasons and in high and low river discharge conditions.

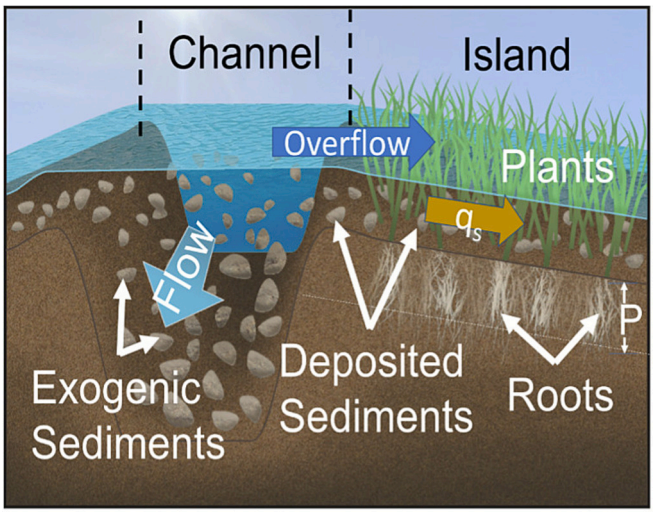

Fig. 2. Soil accretion is dominated by two processes: 1) deposition of mineral sediments delivered by the distributary channel network at a rate, q_s; and 2) accumulation of organic matter (P) generated by local plant growth (roots and litter).

3. The Delta-X framework

3.1. Overview

Hydrodynamic models available today can resolve channels, islands, and vegetation thereby enabling in principle detailed predictions of the response of deltas to RSLR at the mesoscale (e.g., [Fagherazzi et al., 2012; Nardin and Edmonds, 2014; Hiatt et al., 2018; Payandeh et al., 2022]). However, these models have large uncertainty in large part because the available calibration data are sparse point measurements (i.e., evaluate Eq. 1 at a single or few locations). This limitation can be addressed with remote sensing through synoptic measurements at the mesoscale to evaluate and refine input parameters of numerical models and reduce and quantify model uncertainties.

The Delta-X framework is designed to generate multiple layers of information that characterize the geophysical, hydrological and ecological conditions of the landscape, to support the development of accurate hydrodynamic and ecogeomorphic models. The general framework applies to deltas in tropical, temperate, and arctic climates. To assemble the disparate information, reduce computation time, and improve each layer's accuracy, we aggregate information into ecogeomorphic cells, which represent spatially homogeneous sections of the landscape. A cell comprises a region characterized by similar geophysical characteristics (e.g., elevation) and vegetation types and structural

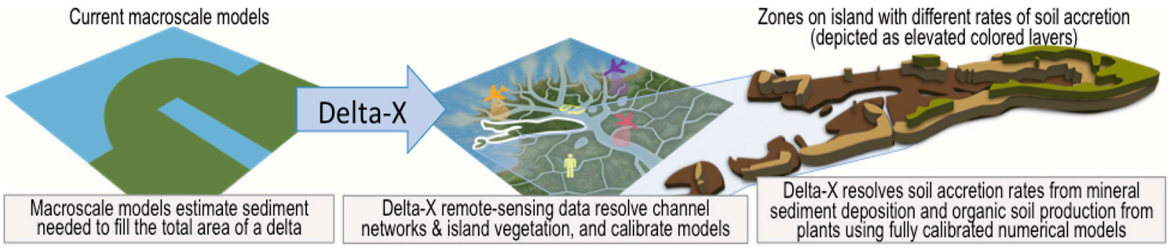

Fig. 1. Delta-X is a cross-disciplinary study encompassing hydrology, ecology, and geomorphology that advances the study of deltaic evolution by resolving land building processes operating at the mesoscale (~1 ha) through calibration and validation of numerical models of hydrodynamic sediment transport, ecological production, and soil accretion with remote-sensing and in situ measurements.

attributes (e.g., biomass, density). These cells are defined from observed ground elevation and remotely sensed observations of land cover characteristics.

The Delta-X framework (Fig. 3) is designed specifically to observe hydrodynamic and ecological processes that control organic and mineral soil accretion at the scale of the ecogeomorphic cells within deltaic islands. Knowledge of where and how much water there is and of how much suspended sediment it carries is critical to calibrate the models. To this end, we identified the information needed to calibrate and validate models to support predictions at these relatively small scales. Table 1 shows the information needed for modeling and their required accuracy. This information can be derived from a combination of remote sensing and in situ measurements, and the Delta-X framework tries to optimize the amount and quality of the information derivable with standard airborne instruments. The sections below describe the remote sensing and in situ measurements, the campaign cadence and observation strategy, and introduces the modeling strategy. Details of the implementation for the Delta-X mission in Louisiana are presented in Section 4.

Table 1
Information needed for models within the Delta-X framework. Requirements shown are targets for planning airborne and in situ collections.

Information	Requirements	Used for…
Spatial distribution of channels	All ≥10 m wide	Hydrodynamic model
Ecogeomorphic cell (EGC)	≥90 % of size ≥1 ha	Hydrodynamic and ecogeomorphic model
Channel-bed topography	Accuracy = Max(10 cm, 3 % of depth)	Hydrodynamic model
Floodplain topography	Accuracy = Max(1 cm, 3 % of depth of flow) averaged over EGCs	Hydrodynamic model
Friction coefficient in channels	Accuracy = ±10 %	Hydrodynamic model
Friction coefficient in vegetation	Accuracy = ±10 %	Hydrodynamic model
Channel-island hydrologic connectivity	Change in water surface elevation between channel and island ≤ 2.5 cm	Hydrodynamic model
Suspended sediment concentration	Accuracy = ±20 % in open water	Hydrodynamic model
Aboveground biomass	Accuracy = ±20 %	Ecogeomorphic model
Belowground biomass	Accuracy = 100 g/m^2 within an EGC	Ecogeomorphic model
Soil Accretion Rate	Accuracy = 0.5 RSLR estimate	Ecogeomorphic model, hydrodynamic model, & final validation of coupled model

3.2. Remote sensing and in situ observations

3.2.1. Airborne remote sensing

The framework uses multi-instrument airborne remote sensing with both fast-repeat and seasonal-repeat measurements. Airborne remote sensing enables repeated measurement of the landscape characteristics at rates significantly faster than the tidal cycle (e.g., hourly or sub-hourly). Furthermore, near-simultaneous measurements with different types of instruments are required to capture the connectivity between channels and wetlands. This combination of simultaneity and rapid repeat makes it practically impossible to obtain the necessary measurements with satellite-borne instruments alone.

Delta-X airborne remote sensing provides spatially extensive estimates of six observables: 1) water surface elevation and 2) slopes in channels and lakes; 3) water surface elevation changes within vegetated areas, i.e., marshes; 4) suspended sediment concentrations in open water; 5) vegetation type; and 6) aboveground biomass. The Delta-X framework as it has been implemented requires two active and one passive sensor, although other options that provide the six datasets listed above could be used if they meet spatial and temporal requirements. The first four observables require imaging from all three instruments flying near simultaneously to observe interacting processes. The last two vegetation observables do not require simultaneous flights if the observations image the same vegetation and growth stage.

The active instruments provide measurements of hydrodynamic processes and the passive instrument measures water turbidity and vegetation properties. One of the active instruments must be a repeat pass InSAR-capable radar for measuring water level change in wetland areas with emergent vegetation with sufficiently rapid repeat imaging to resolve changes in flow in the wetlands across the tidal cycle [Oliver-Cabrera et al., 2021]. The repeat pass SAR must be able to penetrate through emergent vegetation to measure water level changes, for which a longer wavelength radar is better (e.g., L-band repeat-pass SAR interferometer). The second active instrument measures the open water characteristics and can be either a lidar or a radar altimeter (e.g., Ka-band SAR single pass interferometer) to determine the water surface elevation and water surface slopes in the channels and lakes with open

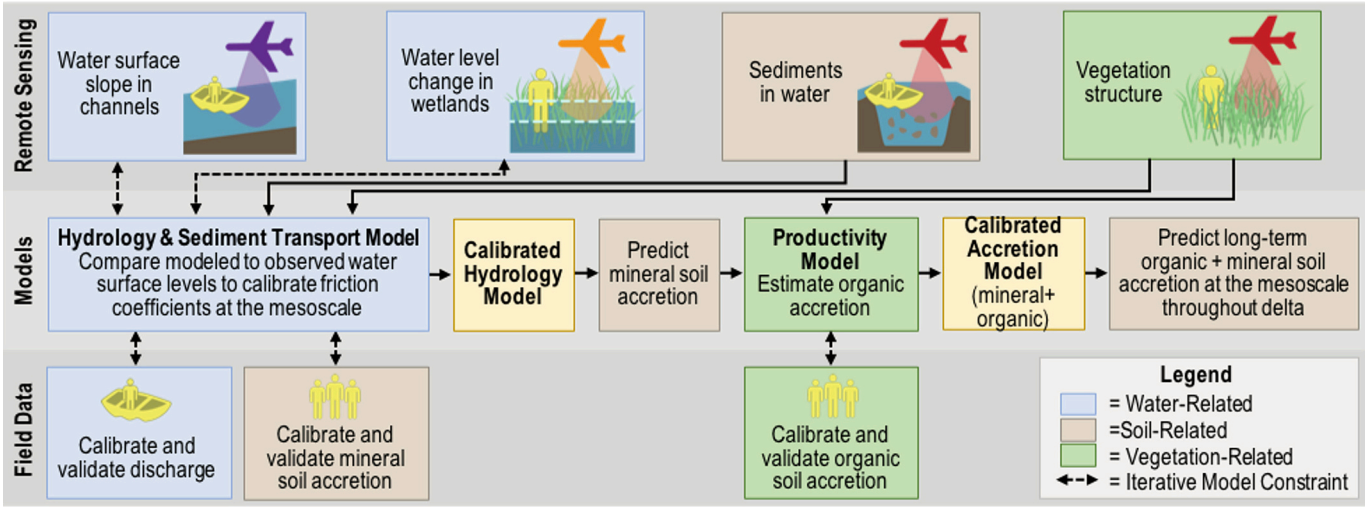

Fig. 3. The Delta-X framework. Delta-X calibrates hydrodynamic, sediment transport, and ecogeomorphic models with remote-sensing and in situ data. Airborne remote sensing instruments provide key spatially extensive information about the vegetation and water channels, flow, and sediment content. In situ measurements calibrate and validate the remote sensing data, provide information for the models, and validate the models' results.

water. The passive instrument is an imaging spectrometer that measures the spectral reflectance of the water and plant surfaces. The water reflectance spectra are directly influenced by the concentration and properties of in-water constituents, including suspended sediments. Vegetation spectra are influenced by canopy structure and chemistry, enabling classification of vegetation types.

The spatial resolution of the SARs is set by the channel size. River deltas form a complex landscape with a large floodplain intersected by curvilinear hydrological and morphological features of scale 5–10 m that should be resolved by the radar remote sensing instruments. Significant distributary channels in river deltas are commonly >10 m wide. This requirement is supported by prior studies, including Delft3D models of flow dynamics at mesoscale resolution (10 m) within channels and wetlands of a salt marsh [Sullivan et al., 2015], and at 18 m resolution for sediment transport following removal of the Elwha Dam in Washington, U.S. [Gelfenbaum et al., 2015].

The needed vertical accuracy of the SARs is set by the tidal range in the delta. For example, the channels in the Delta-X study area can be very shallow with water surface slopes of only a few centimeters per kilometer. Therefore, the altimeter used to measure water surface slope along channels should have centimeter-level accuracy when averaged along the channel reaches. In wetlands, the hydrogeomorphic zones are defined by vertical elevation ranges of ~30 cm [Twilley et al., 2019a, 2019b] and require a precision better than about 15 cm to resolve variations in hydrologic processes affecting these zones. However, this accuracy may not be sufficient to resolve levees and overflows, or other shallow inundation patterns below vegetation. To capture tidal overflows, remotely sensed measurements of water surface change should be a fraction of the tidal range. In a micro-tidal regime, this means the repeat pass SAR should resolve a few centimeters in the vertical direction.

3.2.2. *In situ measurements*

Integral to the Delta-X framework are in situ measurements facilitating calibration of remote sensing measurements and models and providing data that cannot be easily determined from remote sensing (e.g., sediment grain size distribution, plant root-to-shoot ratios). The data collected for Delta-X shown in Table 2 serve as a good example of the types of information that should be collected during in situ campaigns and how it is used within the framework. Intensive study sites at which the complete complement of in situ measurements are made should be set up in different hydrogeomorphic zones and in areas with significantly different sediment input and vegetation structure (i.e., forest vs. marsh).

Ground-based measurements of water level, discharge, flow velocity, and suspended sediment concentration must be collected during the aircraft overflights to calibrate the airborne radar and imaging spectrometer measurements. Vegetation and soil accretion data must be collected during the same seasons as the flights. The collected data include decomposition rates, organic and inorganic packing densities, sediment mass accumulation rates, vegetation's lignin and cellulose content, and root-depth attenuation coefficients used in the development of the organic productivity model. This in situ data also provide above- and below-ground biomass and vegetation structural attributes to calibrate the imaging spectrometer observations of vegetation. In addition, the short-term multi-year (< 4 years) surface soil accretion-rate measurements are needed to validate the inorganic sediment deposition and the final output of the combined hydrodynamic+ecogeomorphic model used for long term prediction. For measurements of soil accretion, e.g., using feldspar layers as marker horizons (e.g., [Cahoon and Turner, 1989; Cassaway et al., 2024]), the feldspar should be deployed at least 6 months before the first airborne campaign, then repeated at least at ~6-month intervals to capture seasonality until after the last campaign is concluded. If possible, additional measurements should be taken after any major disruptive event like a hurricane. The longer the time series, the better the data to support the soil accretion model.

Table 2
Field measurements made for Delta-X.

Field Measurement	Spring 2021	Fall 2021	Used for…
Water level gauges	Collected	Collected	Validate water levels from radar remote sensing. Validate hydrodynamic model.
Global Positioning System (GPS) survey	*Not collected*	Collected	Digital Elevation Model (DEM)
Sonar	*Not collected*	Collected	DEM
Total suspended sediments (TSS) concentration from discrete water samples	Collected	Collected	Train local optical algorithms and validate spectrometer retrievals. Initiate morphodynamic model.
Particulate organic carbon (POC) concentrations from discrete water samples	Collected	Collected	Train local optical algorithms and validate spectrometer retrievals.
Water quality indicators from in situ sonde (Salinity, Temperature, Turbidity, Chlorophyll-a fluorescence)	Collected	Collected	Develop proxy for TSS concentration, train local optical algorithms and validate spectrometer retrievals, determine water types (e.g., freshwater vs. saline, high vs low biomass).
In situ remote-sensing reflectance $Rrs(\lambda)$ of water (above-water field spectrometry)	Collected	Collected	Train local optical algorithms and validate spectrometer retrievals.
In situ beam attenuation and particle size distribution (LISST-200×)	Collected	Collected	Characterize suspended sediment size distribution, settling velocity. Validate sediment transport model
Vegetation structure and above- and belowground biomass	Collected	Collected	Ecogeomorphic model (NUMAR) input parameters. Calibrate and validate spectrometer retrievals of vegetation type and biomass
Sediment core	Collected	Collected	Calibrate NUMAR model
Short-term surface soil accretion from feldspar plots	Collected	Collected	NUMAR model input parameters
Turbidity sensor and water level logger in islands and channel edges	Collected	Collected	Validate morphodynamic model
Suspended and bed-sediment samples for concentration and grain size	Collected	Collected	Calibrate morphodynamics model
Fallout radionuclide (^{137}Cs)	*Not collected*	Collected	Validate NUMAR simulated accretion rates

3.2.3. *Digital elevation model (DEM)*

An accurate topobathymetric DEM representing the land elevation and channel and lake bathymetry is critical for hydrodynamic modeling. In some cases, all or part of this information is available from public sources (e.g., U.S. Geological Survey (USGS) and National Oceanic and Atmospheric Administration (NOAA) for the United States). If necessary, topography and bathymetry can be measured with an airborne lidar that combines near-infrared (NIR) and green lasers to get the desired coverage and spatial resolution, with more sparse topographic calibration data supplied by ground-based lidar, Global Navigation Satellite System (GNSS), or leveling surveys. Channel and nearshore bathymetry can be improved and expanded using a sonar and real time kinematic GPS (RTK-GPS) along boat or foot transects.

3.3. Campaign cadence and observation timing

The Delta-X framework requires cadenced observations on the two timescales that control organic soil production and the net flux of water and sediment within a delta: 1) seasonal cycles of organic production during high and low river discharge; and 2) tidal cycles, which change flows and water levels within channels and wetlands on timescales of minutes to hours. Repeated measurements that span these timescales provide the full range of parameters necessary for model calibration.

Two separate campaigns of coincident airborne and in situ data collection in consecutive spring and fall seasons are necessary to measure changes in vegetation biomass and its impact on flow, and to measure hydrologic connectivity in conditions of high and low discharge, which impacts overbank flow. The consecutive high/low river discharge observations are needed to map sediment and water flow and soil accretion across a yearly cycle of river discharge since it can vary substantially from year to year. The two campaigns with this timing are also needed because the spring river discharge establishes the initial riverine input for the year's organic productivity, hence the necessarily related vegetation growth and dieback during the annual growth season.

In each hydrogeomorphic zone, the spatial pattern of change in water level across a tidal cycle is governed by topography and channel-bed and vegetation friction coefficients [Nardin and Edmonds, 2014; Jalonen et al., 2015; Hiatt and Passalacqua, 2017; Christensen et al., 2020]. Within each campaign, cadenced observations with the two radars in 2.5-to-3.5 h flights of repeated swaths are required to measure tidal water-level change in vegetated floodplains. In each flight, the radar observations are ideally repeated at intervals from 20 min to a few hours to adequately resolve tidal flows and propagation through the channel networks and wetlands. These observations are used by the hydrodynamic model to estimate friction coefficients and water and sediment flux at the mesoscale (i.e., hectare scale). This near-simultaneous measurement of water surface elevation and slopes in river channels with one radar instrument and the associated water level changes within the wetlands with the other are also used to obtain information on channel and wetland flow rates, channel-island connectivity, and water residence time. In situ water level and current measurements must be acquired simultaneously with these flights.

Ideally, imaging spectroscopy measurements conducted over open waters are made coincidently with in situ measurements to provide reliable calibrations and validations of the remote sensing retrievals, although a $\pm$1.5 h window is generally acceptable in tidal systems. Both soil surface accretion measurements using the feldspar technique and the spectrometer measurements of vegetation can be done out-of-sync with the radars and the vegetation-related in situ acquisitions if they occur within a few weeks of each other, dependent on the growth and phenology in the specific study area.

3.4. Models

The Delta-X framework includes models that are calibrated and validated with remote sensing and in situ measurements.

3.4.1. Hydrodynamic model

The choice of numerical model is guided by the need to accurately capture key physical processes across relevant spatial and temporal scales, while also meeting computational constraints. A central requirement is the ability to couple hydrodynamics with sediment and morphological processes to estimate inorganic accretion rates. Our team experimented with the ANUGA implementation [Roberts et al., 2015], which solves the shallow water equations on a flexible mesh. However, the Delta-X implementation of ANUGA [Wright et al., 2022] requires the development of a sophisticated sediment transport module that runs on top of ANUGA hydrodynamic outputs [Wang et al., 2023], which was computationally too intensive to model the entire domain.

To assess the sensitivity of our models to grid size, we conducted a sensitivity analysis using the Delft3D 4 suite, which employs a regular grid. We ran two simulations with spatial resolutions of 30 m and 90 m and compared the amplitude of the K1 tidal harmonic to evaluate how tides propagate in each case. The results (Fig. 4) show that the 30 m model captures diurnal tidal flow penetrating deeper into islands and through smaller channels, while the 90 m model misses much of this fine-scale connectivity. Because it is important to include small channels in the model, it is preferable to use a flexible mesh model to reduce computation resources needed to model the large open water bodies or other features that require less resolution, thus optimizing both accuracy and efficiency. Therefore, for the full domain model we used Delft3D FM for its advanced unstructured grid capabilities, fully integrated hydrodynamic, wave, and morphodynamic modules, and efficient parallel processing performance in simulating complex coastal and estuarine dynamics [Deltares, 2021a, 2021b]. The hydrodynamic module within Delft3D is based on the Navier-Stokes equations under the shallow water approximation, and the morphodynamic module solves the advection-diffusion equation to model the suspended transport for both cohesive and non-cohesive sediment fractions influenced by waves and currents [Deltares, 2021b]. Delft3D requires several input layers such a topo-bathymetric DEM, a map of friction coefficients, and sediment characteristics. These layers are described in Section 5.1.

3.4.2. Ecogeomorphic model (NUMAR)

Delta-X uses an improved and adapted version of the Mangrove Nutrient Model (NUMAN [Chen and Twilley, 1999]), termed NUMAR or Numerical Understanding of Marsh Accretion Rates [Fontenot, 2022; Biswas, 2024] to predict multi-decadal scale soil accretion rates in coastal marshes. Improvements to NUMAN include revised mass balance formulation and reparameterization using Delta-X field measurements [Fontenot, 2022; Biswas, 2024; Cassaway et al., 2024]. The model, shown schematically in Fig. 5, accounts for the annual contribution of inorganic and organic sediment to the surface (mineral sedimentation plus plant-litter accumulation) and subsurface organic production (root turnover) that results in soil volumetric and accretionary changes (mm/y) [Morris and Bowden, 1986; French, 1993; Callaway et al., 1996; Chen and Twilley, 1999; Day Jr et al., 1999; Mudd et al., 2009; Fagherazzi et al., 2012; Morris et al., 2016]. To simulate annual accretion rates, model algorithms account for both surface and subsurface processes, which are essential components to net surface elevation changes in the top 1 m of soil. These processes include the following: 1) annual rate of mineral sedimentation to soil surface; 2) annual rate of organic sedimentation to soil surface; 3) distribution of roots within the sediment column and belowground production associated with biomass distribution within defined rooting depth; 4) the annual production of necromass from root turnover process; and 5) the mass loss through associated decomposition of labile and refractory organic matter that is incorporated into the sediment matrix and contributes to volumetric change [Chen and Twilley, 1999; Mudd et al., 2009; Morris et al., 2016]. NUMAN [Chen and Twilley, 1999] took only lignin into account as refractory organic materials, but NUMAR considers cellulose as a sub-pool of refractory organic matter. Additionally, according to the nature of marsh live roots, it considers no live root biomass beyond the defined rooting depth. NUMAR adjusts the annual contribution of mineral and organic (surface and subsurface) matter to soil volume by building a cohort of sediment elevation each year (sediment cohort model approach). The inorganic mass accumulation rate on the surface is held constant for the defined simulation timeline. As the cohort evolves, root (live and necro root) adds organic matter to the cohort. At the same time, organic (refractory and labile components) matter undergoes decomposition. These processes account for the mass balance as older soil cohorts evolve with depth while new soil cohorts are formed above.

Input model parameters for each cohort include inorganic and organic matter loading rates (si, oms), self-packing density of inorganic and organic matter (bi, bo), lignin content of surface deposits and fine roots (c0, fc1), ash content of biomass (c1), cellulose content of surface

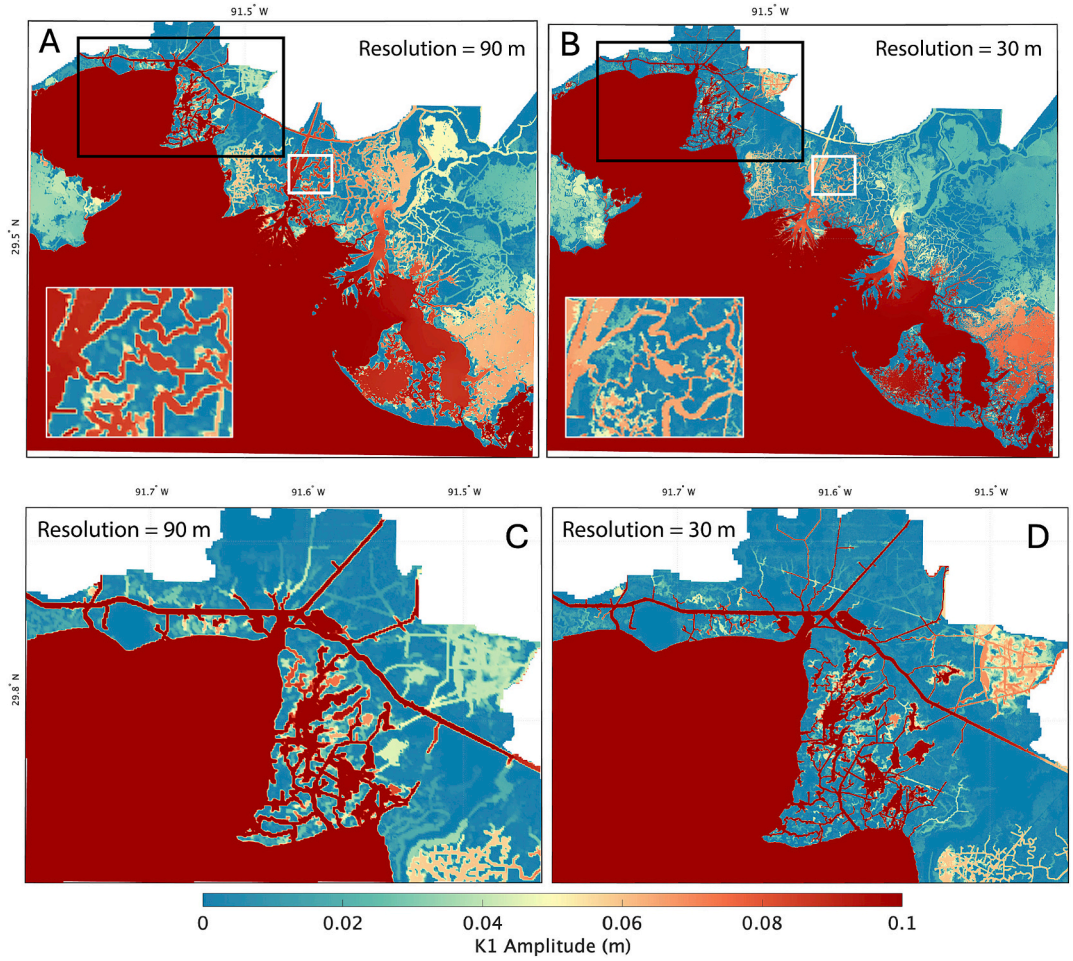

Fig. 4. Comparison between Delft3D results for the K1 tidal amplitude for models with 90 m grid spacing (left) and 30-m grid spacing (right). The inset in A/B are for the area outlined in white, and C/D shows the area outlined in black in A/B. The 30 m grid results show substantially more damping of the tidal amplitude with distance from the open ocean and more extensive water distribution within the interior wetland islands.

deposits and biomass (c2, c4), root distribution (e), belowground decomposition rate of labile organic matter (kb), cellulose and lignin decomposition rates (kc, kl), fine root turnover rate (kr), and live root biomass at the surface (r0). A soil column is constructed over multiple annual cohorts to estimate an elevation at the end of that time period that represents the annual accretion rate from the cumulative integration of mineral and organic sediment input. (Note that NUMAR is intended to show accumulation over decades, not merely a few years.) The Delta-X framework provides the calibration and validation data for the NUMAR model (Table 2; Section 4.2.2 and 4.2.3). Sensitivity analyses have demonstrated that mineral sediment input and root biomass and decomposition are the most important parameters in accurate accretion estimates (±10 %) [Chen and Twilley, 1999]. Both are measured within the Delta-X framework (mineral sedimentation rates and biomass productivity of vegetation).

It is worth noting that land subsidence is in many deltas a critical, possibly driving component of RSLR. That information can take years to obtain so accurate measurements fall outside the Delta-X framework. However, the initial compaction and oxidation of organic soils is included in the NUMAR model. Deeper subsidence must be included separately when comparing modeled accretion to expected RSLR.

4. Delta-X implementation

The Delta-X mission studies the processes controlling land loss and gain within the Mississippi River Delta (MRD), which is one of the largest temperate deltas in the world. The details of the framework's implementation for Delta-X are provided here as a practical example of the complexity of the field and airborne data collections and analyses.

The part of the MRD selected as the Delta-X study site (Fig. 6) contains both an actively growing delta (Wax Lake Delta and the lower Atchafalaya basin) [Roberts, 1997] and the adjacent Terrebonne basin, an inactive, river-abandoned wetland that is part of the formerly active Lafourche Delta Complex of the Mississippi River. At the time of the Delta-X mission, the Terrebonne basin had long been cut off entirely from external sediment input by levees along the Gulf Intracoastal Waterway at the northern boundary and was the site of some of the most rapid wetland loss in Louisiana [Couvillion et al., 2011; Roy et al., 2020; Jensen et al., 2022]. Both areas were otherwise largely unaffected by human activities, and their near proximity allowed controlling for external factors of climate and weather. The geophysical setting in the Mississippi River Delta occurs over a limited range of climatic and vegetative conditions, but it offers a large range of channel configurations and flow conditions due to the high variability in topography and seasonal discharge. Moreover, the framework and parameters calibrated in the Mississippi River Delta are broadly applicable to ~20 % of the major deltas worldwide through the derived productivity relationships and friction coefficient for temperate vegetation types.

Fig. 6 shows the Delta-X study area and the location of the six intensive study sites at which comprehensive field data were collected and used to calibrate and validate the NUMAR model and the combined eco-hydrogeomorphic model. The sites were selected to include

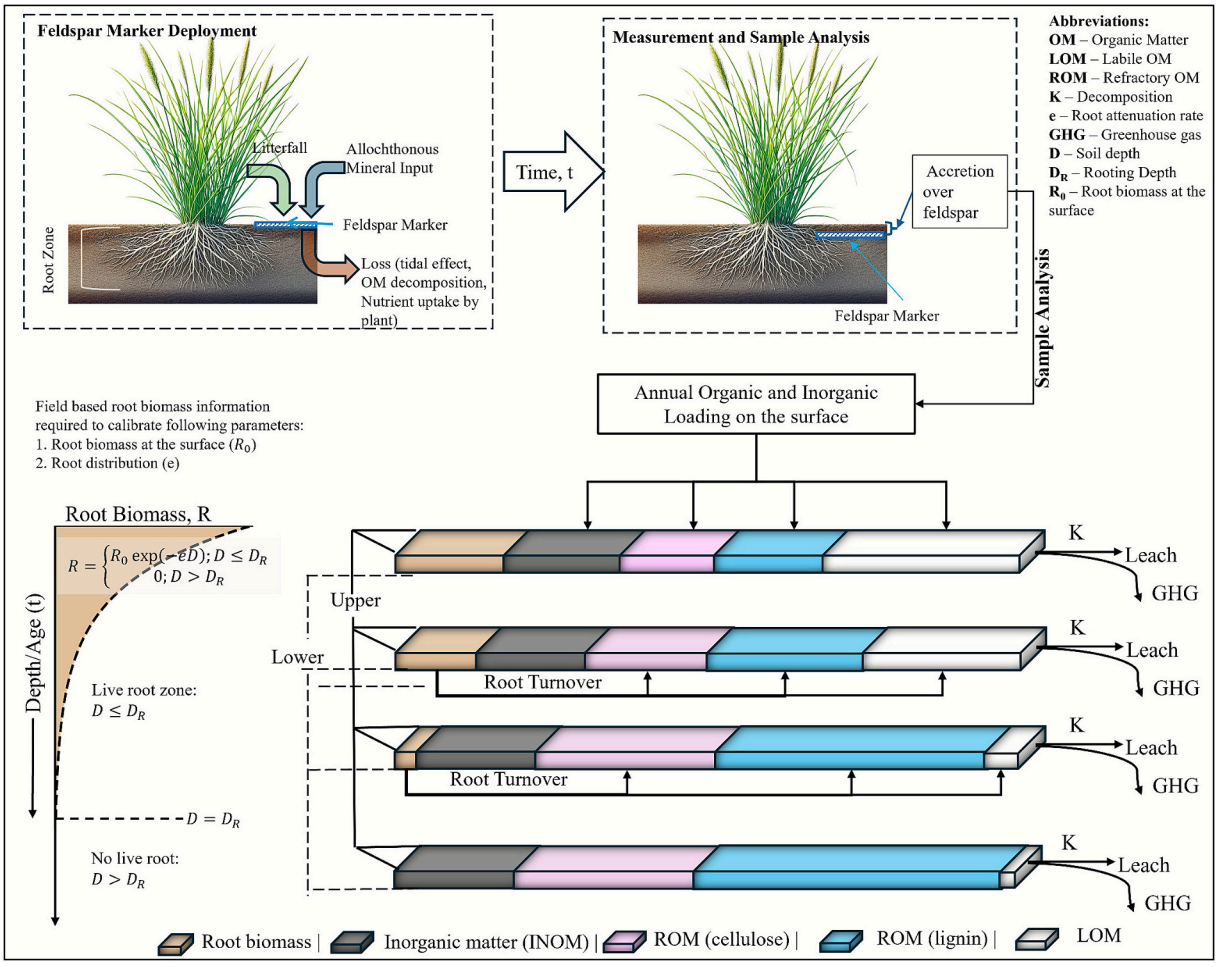

Fig. 5. Schematic conceptual diagram of NUMAR model framework starting from the feldspar marker deployment and flowing down to the cohort model.

Fig. 6. Overview of the Delta-X study area with the Atchafalaya basin outlined in blue and the Terrebonne basin outlined in red. The white circles identify the Wax Lake Delta (west) and the Atchafalaya Delta (east). Delta-X intensive study sites are indicated by stars. The intensive study sites are named for the closest Coastwide Reference Monitoring System (CRMS) station (www.lacoast.gov/crms/; [Steyer et al. 2003]), except for the Wax Lake Delta site, which is located on Mike Island. (For interpretation of the references to colour in this figure legend, the reader is referred to the web version of this article.)

freshwater, brackish, and saline wetlands in the active (Atchafalaya) and inactive (Terrebonne) parts of the study area and located near collection sites of Louisiana's Coastwide Reference Monitoring System (CRMS). Intensive and long-term measurements of vegetation, soil accumulation, and water levels have been made at the CRMS sites and are publicly available [Coastal Protection and Restoration Authority (CPRA) of Louisiana, 2023].

The in situ and remote sensing data collection components of the Delta-X mission were implemented through airborne and field deployments during Spring 2021 (March 21 – April 22) and Fall 2021 (Aug. 16 - Sept. 25). These periods correspond to high and low discharge of the Mississippi River (Fig. 7) and coincide with extremes in plant phenology since the marshes reach peak aboveground biomass in August. Multiple flights in each season covered different stages of the tidal cycle to observe how the tides influenced water and sediment flow through the wetlands (Fig. 7).

Table 1 gives the scientific information requirements from which the in situ data (Table 2) and remote sensing observation requirements are derived and the Delta-X campaigns designed. Delta-X was implemented using three NASA Airborne Science instruments—AirSWOT as the radar altimeter (single pass synthetic aperture radar (SAR) interferometer) [Denbina et al., 2019], UAVSAR for the repeat pass SAR interferometer [Fore et al., 2015], and AVIRIS-NG as the imaging spectrometer [Jensen et al., 2017; Chapman et al., 2019; Harringmeyer et al., 2024], all mature airborne instruments whose deployment was routine on known platforms. Fig. 8 shows the flight lines for each instrument. The study region was separated into three different areas for the purpose of radar imaging so that the individual lines in each area could be acquired a sufficient number of times to observe the tide-induced changes in water within the channels during each ~5 h flight. The areas are the Atchafalaya basin (AT), west Terrebonne basin (WT), and east Terrebonne basin (ET). This permitted each line to be imaged 3–4 times per flight for AirSWOT and 4–9 times per flight for UAVSAR. Multiple images acquired in a single flight are used to track water flow within the wetlands across different parts of the tidal cycle.

The Delta-X Science Traceability Matrix is included in Supplement

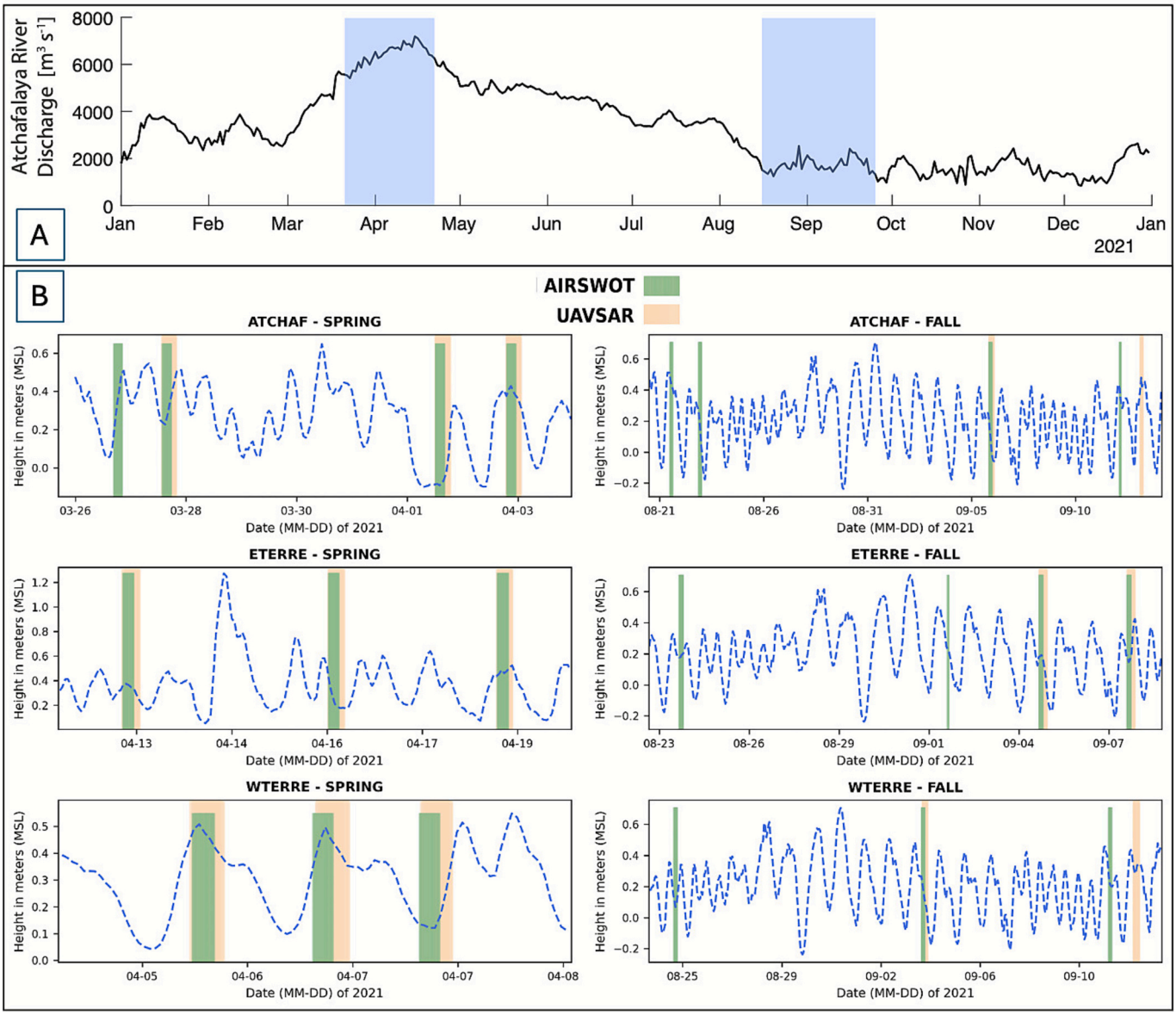

Fig. 7. (A) Discharge for 2021 measured at the USGS Atchafalaya River Gauge in Morgan City, LA. The blue blocks indicated the Delta-X spring and fall campaign periods. (B) UAVSAR (orange) and AirSWOT (green) flight times overlaid on the water level measured at the NOAA Amerada Pass station. (For interpretation of the references to colour in this figure legend, the reader is referred to the web version of this article.)

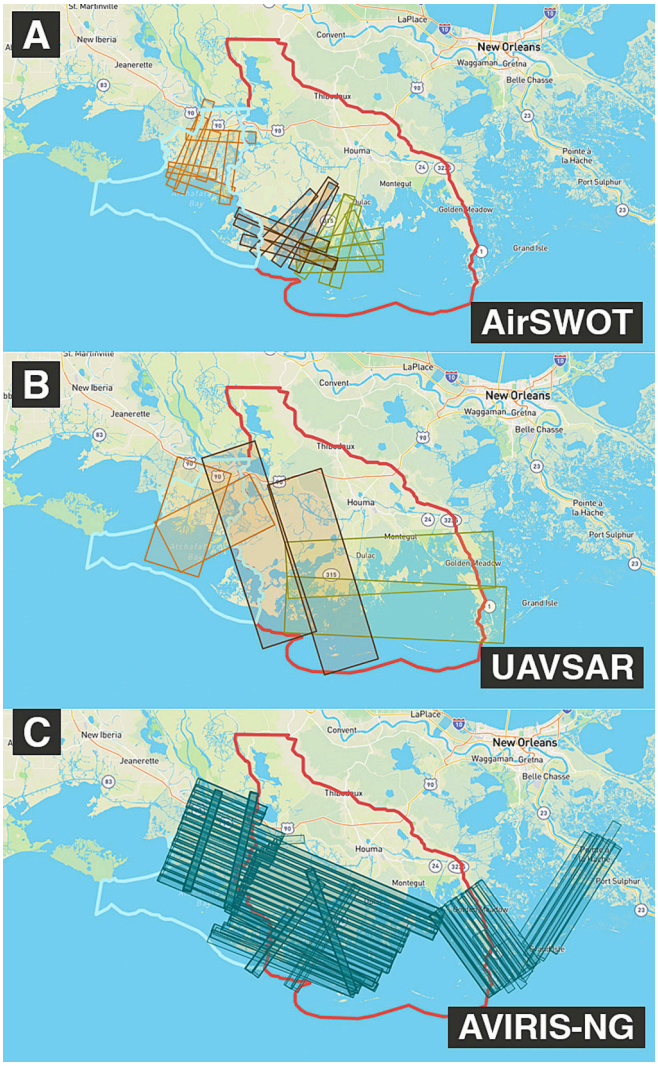

Fig. 8. Flight lines for (A) AirSWOT, (B) UAVSAR, and (C) AVIRIS-NG. The study region was separated into three different areas for the purpose of radar imaging (AirSWOT and UAVSAR), namely the Atchafalaya basin (AT, orange in A,B), west Terrebonne basin (WT, brown in A,B), and east Terrebonne basin (ET, green in A,B). For UAVSAR, line orientation and length at the southern margin was constrained by the requirement that the Gulfstream-3 plane not enter military-controlled airspace in the Gulf of Mexico at any time during flight, including entering, exiting, and transiting between lines. (For interpretation of the references to colour in this figure legend, the reader is referred to the web version of this article.)

Table S-1 and shows the flow from science hypotheses to science goals and objectives, scientific measurement requirements, instrument requirements and performance, and mission functional requirements. All the Delta-X airborne and field data, derived products used in the models, and the models themselves are archived at the Oak Ridge National Laboratory (ORNL) Distributed Active Archive Center (DAAC) [https://daac.ornl.gov/get_data/]. Each dataset is accompanied by a document explaining the acquisition and analysis method. In addition, tutorials for using the data and the models developed for Delta-X Applications Workshops are accessible through ORNL DAAC. Development of the EVS-3 Delta-X proposal was supported by two airborne campaigns in 2015 and 2016 (Pre-Delta-X campaigns), and those relevant data and science products are also available at the ORNL DAAC. Field data is designated Level-0 (L0), NASA's denotation for raw data. The airborne data are available as Level-1 (L1, low-level processed data in instrument coordinates, e.g., interferograms for the radars), Level-2 (L2, geocoded derived data), and Level-3 (L3, information derived from the L2 data). Additional information about the airborne and field sensors, measurements, methods, and models are given in the sections below.

4.1. Airborne remote sensing

4.1.1. AirSWOT

AirSWOT is a Ka-band (35.75 GHz) single-pass radar interferometer for measuring water surface elevation [Denbina et al., 2019]. AirSWOT radar measurements have a spatial resolution of 2–3 m and cover a cross-track swath of 4 km, though the usable swath is closer to 3 km, yielding 1) a height accuracy of 12 cm root mean square error (RMSE) for water-surface elevation, averaged over 0.5 km^2 area; and 2) a slope accuracy of <1 cm/km over a 10 km stretch of channel. The height accuracy was validated by comparing AirSWOT to in situ gauge data by averaging open water AirSWOT pixels within a 0.5 km^2 circular area around each gauge.

During Delta-X, the AirSWOT flights were conducted concurrently with the UAVSAR flights whenever possible, and the field crews deployed to collect water data concurrently insofar as possible. The AirSWOT image swaths are shown in Fig. 8A and information about the instrument and acquisitions are in Table 3. AirSWOT acquired data along the main channels in the Atchafalaya and Terrebonne study areas, plus crossing lines that imaged additional open water and small channels and were used for calibration in the AirSWOT operational data processor. AirSWOT measurements were calibrated using a mixture of relative calibration by "flattening" erroneous cross-track slopes within the crossover areas, as well as absolute calibration using specific in situ gauges (one for each basin) which were then excluded from validation. Phase calibration coefficients were estimated using a weighted least squares solution that attempted to minimize discrepancies between crossovers and with the gauge data. The calibration method is presented in detail in Denbina et al. [2019]. Fig. 7B shows the tidal conditions during the times when AirSWOT data were acquired in both spring and fall 2021, and Fig. 9 shows an example of the channel water surface elevation measured by AirSWOT. In spring, there were at least three flights per area, ideally to image near high tide, low tide, and either rising or falling tide. In fall, the goal was to collect near high and low tide, i.e., only two flights per area because the river discharge was low. In practice, flight departure and return times were largely set by the weather, which affected when field crews could be in the areas (e.g., to avoid lightning strikes) and when the aircraft could safely take off, fly, and land. As Fig. 7B shows, these constraints made it impossible to image the ideal tidal conditions. Also, in fall the AirSWOT flights were done twice, once before Hurricane Ida made landfall at the east edge of the study site on Aug. 29, 2021, and once afterwards, when UAVSAR was available to support the Delta-X campaign.

AirSWOT data are used to derive the L3 Water Surface Elevations product [Denbina et al., 2022], which contains water surface elevations at selected point locations, e.g., to show the profile along a channel as in Fig. 9. The lower-level products from which this information is derived are also available, namely the L1 Interferograms [Denbina et al., 2021] and the L2 Geocoded Water Surface Elevation maps showing the derived water surface elevation across the full extent of each swath shown in Fig. 8A [Denbina et al., 2023].

4.1.2. UAVSAR

UAVSAR is an L-band (1217.5–1297.5 MHz) polarimetric SAR deployed on a Gulfsteam-3 jet that can operate transmitting and receiving either horizontal (H) or vertical (V) polarized pulses. UAVSAR's spatial resolution is 1.8 m (slant range) by 0.8 m (azimuth) for single-look complex products (L1), and the multilooked, georeferenced products (L2) have a 5.5 m posting. UAVSAR's performance and calibration method are described by Fore et al. [2015]. During the Delta-X campaigns, the UAVSAR instrument was operated in its standard acquisition configuration at an altitude of 12.5 km in quad-polarization

Table 3
Delta-X airborne instruments, acquisitions, and derived information. The spatial resolution of the AirSWOT and AVIRIS-NG instruments is 5 m. UAVSAR geocoded products are generated with ~6 m pixel spacing.

Instrument	Sensor type	Swath width	Measurement	Spring 2021 campaign dates	Fall 2021 campaign dates	# of Lines	# of Flights
AirSWOT	Ka-Band (35.75 GHz) single pass interferometer	4 km	• Open water surface elevation and slope	March 26 – April 18	Aug. 21 – Sept. 12	Spring: 222 Fall: 189	Spring: 10 Fall: 11
UAVSAR	L-band quad-polarimetric synthetic aperture radar repeat pass interferometer (80 MHz bandwidth)	21 km	• Water surface level change in marshes and swamps. • Channel network mapping	March 27 – April 18	Sept. 1 – Sept. 12	Spring: 137 Fall: 83	Spring: 9 Fall: 7
AVIRIS-NG	Imaging spectrometer (425 bands 380–2510 nm, 5 nm spectral resolution)	3.2 km	• Total suspended sediments concentration • Vegetation type • Aboveground biomass	March 27 – April 6	Aug. 18 – Aug. 25	Spring: 76 Fall: 69*	Spring: 6 Fall: 6

* AVIRIS-NG flew three additional flights after Hurricane Ida and collected 56 lines.

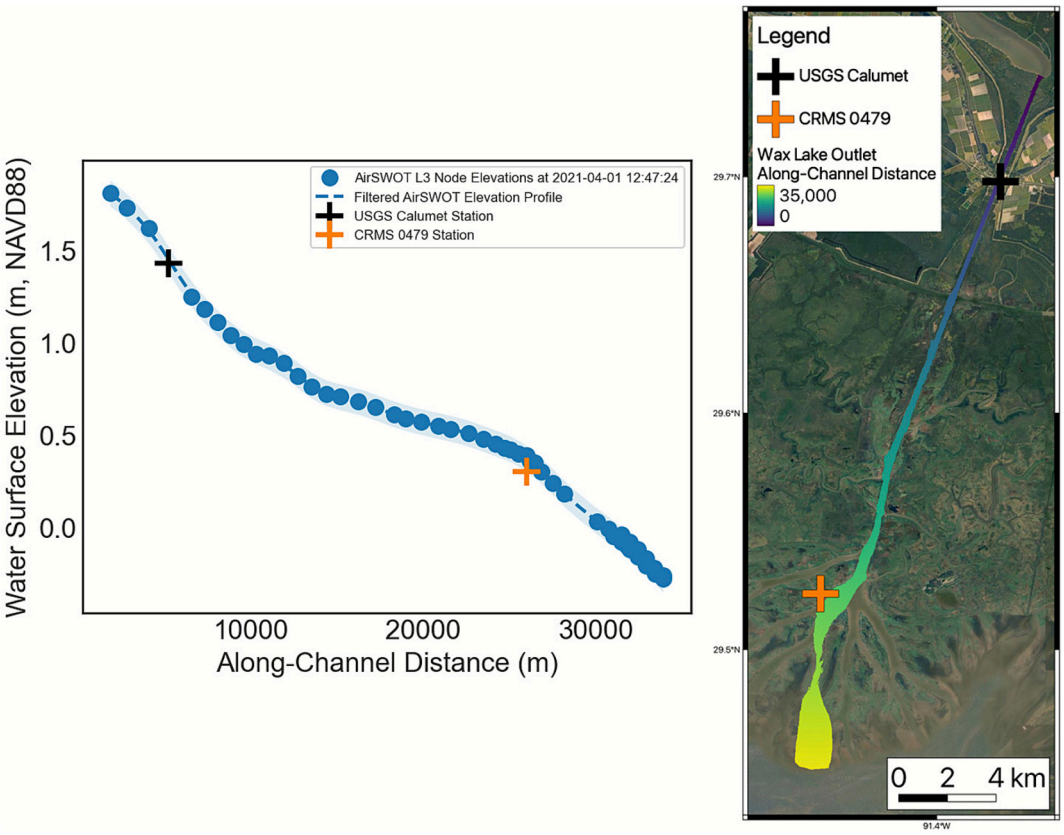

Fig. 9. Water surface elevation along the Wax Lake Outlet from AirSWOT data acquired on 4/1/2021 during the spring Delta-X campaign [Denbina et al., 2022]. The water levels recorded by the USGS Calumet and CRMS 0479 gauges at the same time are shown for reference. On the right, a map shows the location of the profile and gauges.

mode, transmitting horizontally and vertically polarized radiation on alternate pulses and receiving both co-polarized (HH or VV) and cross-polarized (HV or VH) returns for each pulse.

The UAVSAR image swaths are shown in Fig. 8B, and information about the instrument and acquisitions are in Table 3. There were six image swaths, two per study area (AT, WT, ET) and during a flight the single pair was flown in a 'racetrack-like' pattern. For UAVSAR, a single wrap of the interferogram corresponds to 11.9 cm of water level change, which can be more than the tidal range, so to avoid ambiguities the repeat times were kept to 20–40 min by plan. Fig. 7B shows the tidal conditions during the times when UAVSAR data were acquired in three flights in spring 2021 and two flights in fall 2021. Fig. 10 shows an example of the water level change measured by UAVSAR. This example shows the turning of the tide in an island of the Wax Lake Delta. Water level change measurements depend on double-bunce scattering, where the radar echo reflects off both the water surface and emergent vegetation. As a result, these measurements are inherently constrained to regions where emergent vegetation is present. While changes in water surface elevation have been observed in wetlands using spaceborne radar [Wdowinski et al., 2004; Liu et al., 2020], it has not been tracked at the timescale of tides before the Delta-X mission [Varugu et al., 2025]. Even the relatively dense distribution of water level gauges across the Mississippi River delta landscapes cannot resolve the spatially complex patterns observed here. The Delta-X water level change values were derived using a new phase unwrapping error correction method designed to work in settings where channels divide the landscape into many islands [Oliver-Cabrera et al., 2021], which achieved a water level change RMSE of 3 cm based on comparison with CRMS water level

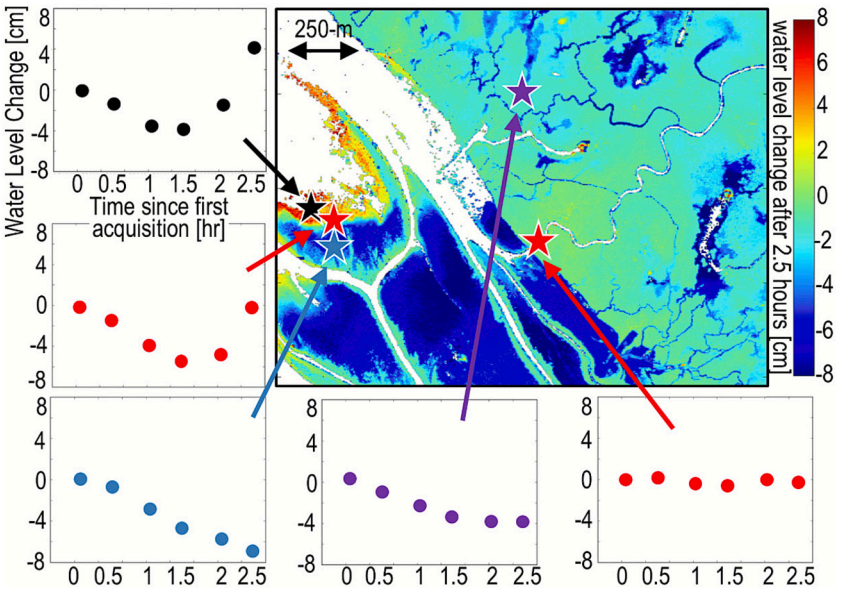

Fig. 10. UAVSAR-derived water level change over a 2.5-h period as the tide was coming into the Wax Lake Delta. Time series are shown at different locations. Plots show how the water propagates across the island and inland along channels, and the change in flow direction at the island margins, but there is no measurable change over much of the more inland wetlands in this short period at low tide. Data are from the Pre-Delta-X campaign in 2016 [Jones et al., 2021].

gauges. Weather radar was used to identify and exclude areas where phase delay from wet troposphere introduced large errors in the derived values [Oliver-Cabrera et al., 2025].

The data available from UAVSAR are the L3 Water Level Change maps [Jones et al., 2022a]; the channel map for the study area showing open water and flow below vegetation [Jones et al., 2024]; Interferometric Products, both georeferenced [Jones et al., 2022b] and in radar coordinates [Jones et al., 2022c]; and the Single Look Complex Stack products [Jones et al., 2022d] that serve as the basis for all the above.

4.1.3. AVIRIS-ng

AVIRIS-NG, the Next Generation Airborne Visible InfraRed Imaging Spectrometer, is a pushbroom imaging spectrometer with high signal-to-noise ratio (SNR) that covers the solar spectral range from 380 to 2510 nm with a single 640 × 480 pixel Focal Plane Array (FPA) at a spectral sampling of approximately 5 nm [Chapman et al., 2019]. For Delta-X, AVIRIS-NG operated on a Dynamic Aviation KingAir B200 aircraft. The AVIRIS- NG sensor has a 1 mrad instantaneous field of view, providing altitude-dependent ground sampling distance ranging from sub-meter to 20 m scales. Each acquisition is a "flight line" forming a continuous strip of pushbroom data that typically takes 1–10 min to acquire. Multiple aircraft overflights cover the region of interest in these strips, accumulating a combined map of the target area. The precise direction of flightlines was adjusted to accommodate local solar position and weather conditions, and to ameliorate sun glint effects.

The AVIRIS-NG flight lines, shown in Fig. 8C, were designed for two distinct applications, namely characterization of vegetation structure [Jensen et al., 2019a] and measuring water quality (e.g., total suspended solids (TSS) concentration) [Jensen et al., 2019b]. The lines for imaging the vegetation were planned to cover large rectangular areas by flying back and forth along adjacent strips to systematically image the entire study area. The water quality flight lines imaged the large and medium sized channels and were flown several times during each campaign to coincide with field measurements of water quality at locations throughout the study area. Flight days were selected to optimize cloud-free coverage, though isolated clouds occasionally appear in the data. On several flight days, a team in the field during the AVIRIS-NG overflight measured representative uniform surfaces with ASD spectroradiometers and atmospheric data with Microtops-2 sunphotometers. A team was also deployed on the water during most flights to measure coincident in-situ remote-sensing reflectance spectra, Rrs(l), of the water surface using a Spectral Evolution® PSR-1100f spectrometer with an above-water approach [Fichot and Harringmeyer, 2023b]. These in situ Rrs(l) were collected concurrently and co-located with measurements of water-quality indicators and sediment properties. The in situ data were used to validate [Harringmeyer et al., 2024] and, where necessary, adjust [Greenberg et al., 2022] AVIRIS-NG L1 and L2 data.

The derived information products available from AVIRIS-NG are the L3 Vegetation Types [Jensen et al., 2024a], Herbaceous Aboveground Biomass, Necromass, and Net Primary Productivity [Jensen et al., 2025a], Forest Aboveground Biomass [Jensen et al., 2025b], Herbaceous Belowground Biomass [Jensen et al., 2025d], and surface-water TSS concentration and Turbidity [Fichot and Harringmeyer, 2023a]. Fig. 11 shows the vegetation type map derived from AVIRIS-NG and Fig. 12 shows the TSS maps for spring and fall. The lower level sensor data are also available, namely: L1 Spectral Radiance [Thompson et al., 2022a], produced using standard approaches detailed in Chapman et al. [2019]; the L2 Surface Reflectance, [Thompson et al., 2022b], produced using techniques detailed in [Thompson et al., 2018, 2019]; L2B BRDF-Adjusted Surface Reflectance and Mosaics [Thompson et al., 2025], with all AVIRIS-NG flightlines further processed with the bidirectional reflectance distribution function (BRDF) and aquatic sunglint adjustments described by Greenberg et al. [2022] and used to produce regional mosaic imagery; and L2B Fractional Cover [Jensen et al., 2025c], quantifying the per-pixel composition of green vegetation, non-photosynthetic vegetation, and soil.

4.2. In situ measurements

The complexity and diversity of measurements needed to address the Delta-X objectives required careful selection of in situ field sites throughout the study domain, including intensive study sites where complete sets of in situ data covering vegetation, hydrology, and soil accretion were acquired. Information about the Delta-X intensive study sites and the in situ data collection and analysis methods are given in subsections below.

4.2.1. Intensive study sites

The intensive study sites were established to collect multiple datasets in herbaceous wetlands with a gradient of surface water salinity and

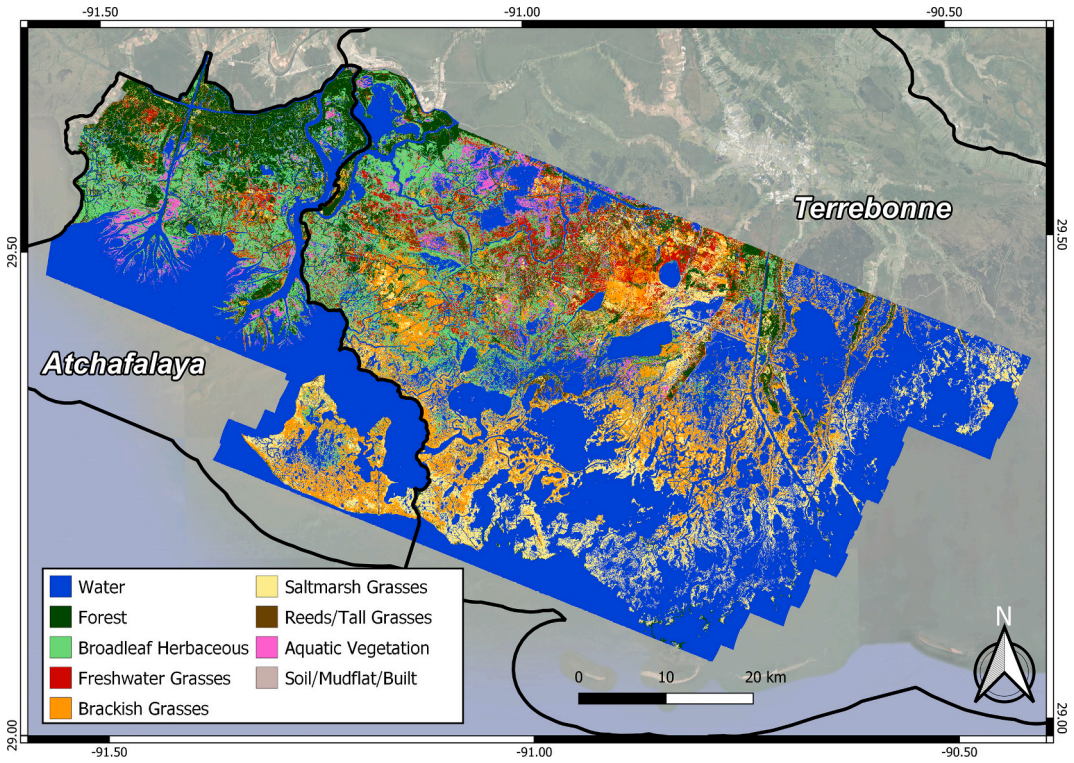

Fig. 11. Map of vegetation type and water derived from AVIRIS-NG data collected during the Spring 2021 and Fall 2021 campaigns [Jensen et al., 2024a].

with or without influx of riverine sediment from upstream. Table 4 provides information about the site characteristics and types of data collected at each intensive site, and Fig. 13 shows the sites' layouts and the acquisitions in the general vicinity of each (in addition to those listed in Table 4). The brackish and saline 'active' sites (CRMS 0399 and CRMS 0322, respectively) are located at the boundary between the Atchafalaya and Terrebonne basins but were included within the active basin due to the documented sediment connection between the Atchafalaya River and Fourleague Bay [Perez et al., 2000; Wellner et al., 2005; Restreppo et al., 2019; J. Wang et al., 2018] Although comprehensive measurements were made at each site, the majority of collections at these sites focused on vegetation and soil properties. The intensive study sites mainly provided the data used in developing the NUMAR model of organic productivity and soil accretion, and to validate remotely sensed estimates of aboveground biomass and modeled accretion rates.

4.2.2. *Vegetation*

Measurements of vegetation characteristics and soil accretion rates were performed only within the six intensive study sites (Fig. 13). Vegetation was sampled in both spring and fall of 2021 to determine above- and belowground biomass and necromass, vegetation structure (e.g., plant stem density), species composition, soil properties (e.g., bulk density, nutrient content) and carbon (13C) and nitrogen (15 N) isotopic signatures of leaves, roots, and soil.

At each herbaceous wetland site, duplicate sampling stations (30 m apart) were established parallel to the wetland edge at 25 and 50 m within the intertidal zone to capture within-site variability in vegetation dynamics and soil properties. In WLD, due to a variety of elevation ranges within the wetland site, duplicate stations were established in the high and intermediate intertidal zones.

At each site, aboveground biomass and necromass were harvested inside duplicate plots (0.25 m^2), located 5 m apart at each sampling station (8 per site). All plant material within each plot was clipped at soil level, stored in plastic bags, and transported to the laboratory for further analyses. In the laboratory, the aboveground vegetation was analyzed to determine species composition, stem diameter, density, and height [Castañeda-Moya and Solohin, 2023a]; biomass and necromass (g m^{-2}) and foliar carbon, nitrogen, and phosphorus content [Castañeda-Moya and Solohin, 2023b], and carbon and nitrogen isotopic signatures for two dominant species at each site [Castañeda-Moya and Solohin, 2023c].

Belowground root biomass and necromass were collected at the same intensive sites. In each sampling station, duplicate (0–50 cm depth) soil cores were collected adjacent to aboveground biomass/necromass plots using a modified soil gouge auger (11-cm diameter x 50-cm length). Soil cores were gently extruded, divided into 10-cm intervals and stored on ice in plastic bags for further analyses. All root core samples were processed separately and initially rinsed with water through a 1 mm synthetic mesh screen to remove soil particles. All roots were separated into live (biomass) and dead (necromass) fractions within 4–6 weeks after collection. Live roots were separated by hand picking those floating in freshwater and were easily distinguished from necromass because of their buoyancy, turgor, and colour. Live roots were sorted into diameter size classes of fine (<2 mm) and coarse (>2 mm) roots. Root data were used to estimate belowground root biomass and necromass (g m^{-2}) and root carbon, nitrogen, and phosphorus content [Castañeda-Moya and Solohin, 2022], and carbon and nitrogen isotopic signatures of living root tissue [Castañeda-Moya and Solohin, 2023d]. The references above contain information about the analysis methods and datasets.

4.2.3. *Soil properties and soil accretion*

For Delta-X, soil accretion measurements to characterize newly deposited soil combined with soil properties from the 50 cm cores were used to develop a model of organic productivity. In fact, multiple bi-yearly measurements of soil accretion across as long a time period as possible are needed to quantify the contributions of organic productivity and inorganic sediment to capture accretion changes across hydrogeomorphic zones. For our purposes, the zones are defined by surface elevation as subtidal < -0.04 m, intertidal -0.04 m to 0.30 m, and supratidal >0.30 m relative to NAVD88 [Bevington and Twilley, 2018]. Given the limited mission duration, we collected the data for ~3.5 years. The feldspar marker horizon technique [Cahoon and Turner, 1989] was

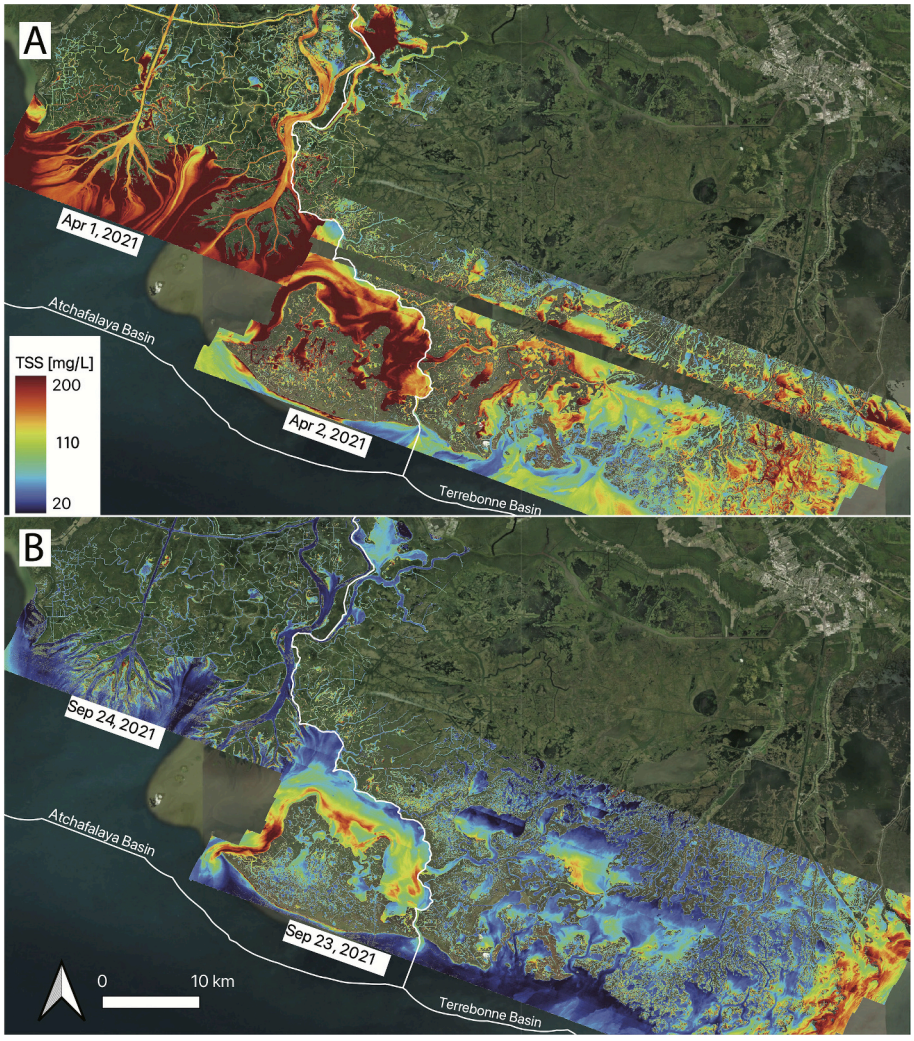

Fig. 12. Total suspended solids (TSS) mapped in the Atchafalaya and Terrebonne Basins from AVIRIS-NG imagery collected on (A) April 1–2, 2021, and (B) September 23–24, 2021, during the spring and fall field campaigns (Harringmeyer et al., 2024).

Table 4
Intensive study site information. Site locations are shown in Fig. 6 and close up images of each site and the surrounding area are shown in Fig. 13. (AGB = above ground biomass, BGB = below ground biomass, AGN = above ground necromass, BGN = below ground necromass, VTS = vegetation type and structure, SA = soil accretion, SP = soil properties, T = turbidity, air temperature and pressure).

Site	Salinity	Exogenous Riverine Sediment?	In Situ Data Acquired
Wax Lake Delta	freshwater	Yes	AGB, AGN, BGB, BGN, VTS, SA, SP, T
CRMS 0399	brackish	Yes	AGB, AGN, BGB, BGN, VTS, SA, SP
CRMS 0322	saline	Yes	AGB, AGN, BGB, BGN, VTS, SA, SP
CRMS 0294	freshwater	No	AGB, AGN, BGB, BGN, VTS, SA, SP
CRMS 0396	brackish	No	AGB, AGN, BGB, BGN, VTS, SA, SP
CRMS 0421	saline	No	AGB, AGN, BGB, BGN, VTS, SA, SP, T

used with markers set up in October 2019 and sampled twice yearly through spring 2023. At each feldspar station, three 50-cm x 50-cm feldspar marker horizons plots were installed. Soil cores using cryo-core methods were collected and analyzed to obtain soil carbon content, bulk density, organic matter content, and total sediment accretion above the marker horizon [Cassaway et al., 2024; Twilley et al., 2024b]. Using a Russian peat corer (5 cm diameter), additional soil cores (50 cm depth; one core per sampling station) were collected at each intensive site nearby feldspar sampling stations to determine below ground biomass, bulk density, organic matter content, and total densities of carbon, nitrogen, and phosphorus within each 10-cm interval [Castañeda-Moya and Solohin, 2023e]. This core dataset provides a longer time history of soil mineral and organic matter composition and nutrient concentrations than that from the soil accreted above the feldspar markers alone.

4.2.4. *Sediment, water quality, and remote sensing Reflectances*

During both Delta-X campaigns, field teams collected samples and data in channels throughout the Atchafalaya and Terrebonne basins, and at numerous sites on Mike Island in the Wax Lake Delta. Fig. 14A shows the locations of the water quality and remote-sensing reflectance measurements made domain-wide, and Figure S-1 shows the locations broken out separately by those collected during the spring and fall because not all locations were revisited. Total suspended solids concentrations (TSS) were measured from surface water samples collected directly from a boat by submerging a 4-L van Dorn sampler about 0.5 m beneath the surface. The volume sampled was then transferred in its entirety into a 4-L amber plastic bottle (HDPE) and kept in a cooler with ice until analysis in the lab within a few hours as described in Harringmeyer et al. [2024]. Data available from these samples include TSS

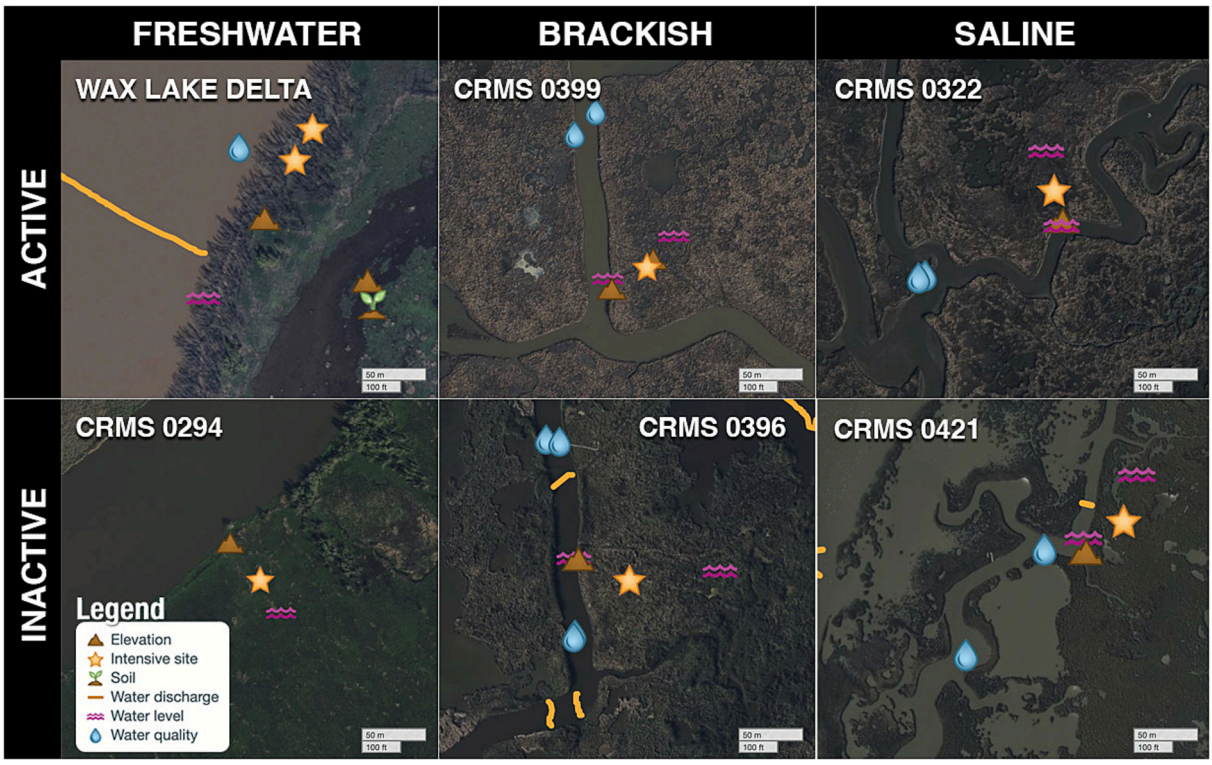

Fig. 13. View of the extensive study sites showing data collected in the immediate vicinity in addition to that listed in Table 4, which were collected at the locations indicated by stars. Labels indicate the salinity and whether the site is in an active or inactive part of the study area. The active brackish and saline sites are located in the Terrebonne basin at the border with the Atchafalaya basin. These sites receive sediment from the Atchafalaya River through Fourleague Bay.

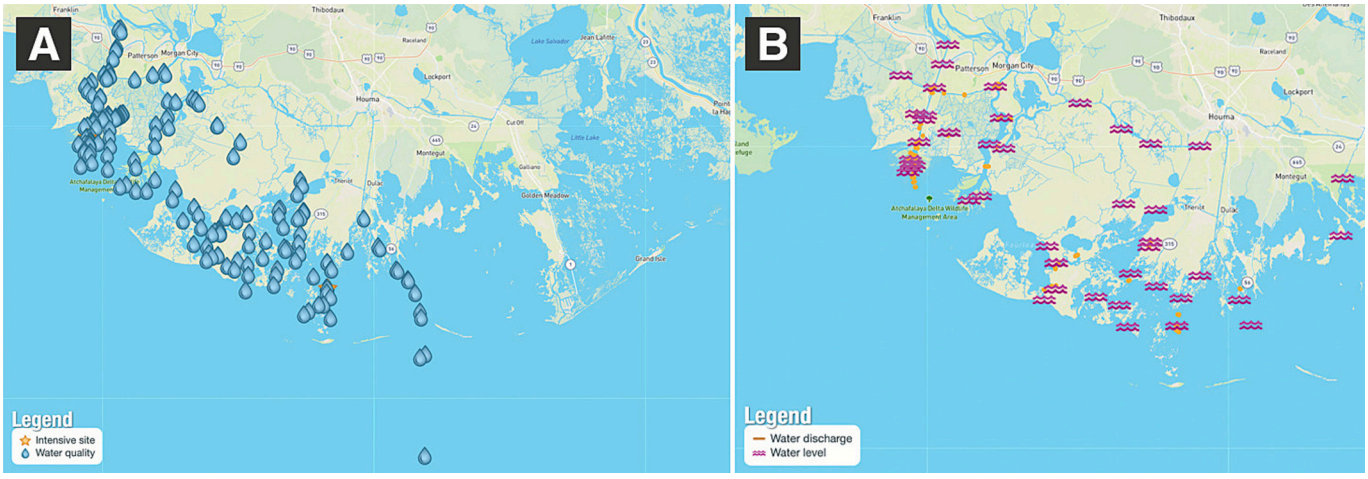

Fig. 14. (A) Sampling sites for water quality parameters. (B) Locations of water level gauges and current profile measurements.

concentration [Fichot et al., 2022a] and particulate organic carbon (POC) concentration [Fichot et al., 2022b]. At most sites, estimates of beam attenuation coefficient at 670 nm, suspended sediment size distribution, and mean Sauter diameter were acquired by using a Sequoia Scientific® LISST-200× (LISST) submersible particle size analyzer [Fichot and Harringmeyer, 2022]. Additionally, water quality indicators of salinity, temperature, turbidity, and chlorophyll-a fluorescence [Fichot et al., 2022c] were also collected using a calibrated YSI® ProDSS sonde (2021-03-25 to 2021-08-14) or a YSI® EXO3 water quality sonde (2021-09-13 to 2021-09-24). Measurements of in situ remote-sensing reflectances were also collected concurrently at these stations using an above-water approach with a Spectral Evolution® PSR-1100f spectrometer [Fichot and Harringmeyer, 2023b; Harringmeyer et al., 2024]. The data were processed and used to develop and validate optical algorithms to facilitate the retrieval of TSS concentration and properties (e.g. POC/TSS) from the AVIRIS-NG imagery [Harringmeyer et al., 2024].

In the Wax Lake Delta and near CRMS 0421, more detailed measurements of sediment concentration-depth profiles and bed material were made to resolve vertical patterns in sediment concentration and grain size distribution in the water column [Nghiem et al., 2023]. Suspended and bed sediment samples were collected from a boat using a van Dorn sampler and a Ponar bed sampler, respectively. ADCP flow velocities were measured concurrently with concentration-depth profiles to give a local estimate of bed shear stress important for sediment transport. In combination, these data allow testing of bed material

entrainment theory for modeling sediment transport in the delta [De Leeuw et al., 2020]. In situ turbidity sensors [Nghiem et al., 2022], once calibrated using in situ suspended sediment samples, yielded time series of sediment concentration coinciding with several water level stations to validate morphodynamic models. A field camera system was also deployed for some concentration-depth profiles in which photos were captured of settling particles to directly measure their size and settling velocities. Combining concentration-depth profile, LISST, and camera data revealed detailed properties of sediment aggregates ("flocs") that are ubiquitously transported throughout the Wax Lake Delta [Nghiem et al., 2024].

4.2.5. Water level and discharge

Fig. 14B shows the locations of the water level and discharge measurements domain-wide. In addition to the CRMS water level stations in the study area, total pressure transducers (TPTs) were installed at 65 locations in channels and inundated wetlands to record water level changes during and between the spring and fall 2021 campaigns. Of these, 6 were lost and 11 corrupted, leaving 48 useful for Delta-X and highlighting the need to plan for loss of these sensors during long-duration measurements. The in situ locations were chosen strategically to cover the geographical domains of the hydrodynamic models, providing measurements in large and small channels, within marshes and swamps, and at locations where AirSWOT swaths overlapped (Fig. 8A), an important constraint for calibrating the water surface elevation data. Five in situ water level stations in Wax Lake Delta and four in Terrebonne also had accompanying turbidity sensors used to estimate sediment concentration time series (Section 4.2.4) [Nghiem, 2022]. In addition to the water level data from the stationary TPT stations, we also performed a GNSS survey from a boat during fall 2021 using a GNSS antenna mounted on a pole directly above the depth sounder to measure water surface elevation [Christensen et al., 2023a].

River discharge was measured using an acoustic doppler current profiler (ADCP) along cross-channel transects in selected wide channels (>100 m wide), some mid-sized channels, and a few narrow channels near the intensive study sites (~10 m wide) (see Fig. 14B) [Christensen et al., 2022a]. Transects were collected during AirSWOT flights, and the same locations were sampled multiple times to collect data during different stages of the tidal cycle. Reported data include bathymetry, discharge (m^3s^{-1}), and flow velocity. Methods to collect and process the data are described by Christensen et al. [2022a].

4.2.6. Topobathymetric DEM

We generated a new topobathymetric digital elevation model for the Delta-X study area [Christensen et al., 2023b] combining publicly available topography and bathymetry elevation data from USGS, NOAA, and CPRA with new data collected during the Delta-X and Pre-Delta-X campaigns. Land and water were classified using Normalized Difference Water Index (NDWI) values derived from the National Agriculture Imagery Program (NAIP). NAIP data are available in 2010, 2013, 2015, 2017, and 2019. For each year, NDWI was calculated using the green and near-infrared bands. A threshold value of 0.1 is used to delineate water and land based on visual interpretation. Pixels that were classified as water for at least 3 out of 5 NAIP years were considered to be permanent open water bodies. The majority of land topography data were derived from the USGS National Elevation Dataset from 2012, 2013, 2015, and 2017 (https://www.usgs.gov/publications/national-elevation-dataset) [Gesch et al., 2002]. Over the WLD, aerial lidar data were collected by the National Center for Airborne Laser Mapping (NCALM) in November 2020 [Nghiem, 2022]. Channel, lake, and bay bathymetry was obtained by combining new sonar bathymetry surveys made in 2021 [Christensen et al., 2022b] with surveys from the Pre-Delta-X campaign [Denbina et al., 2020], USGS [Kroes, 2022], NOAA [Love et al., 2012], and CPRA [Water Institute of the Gulf (Water Institute), 2019; Folse et al., 2020]. For water bodies larger than 1 ha without reliable bathymetry data, elevations are set to -2 m NAVD88. The method used to combine the data is described in Christensen et al. [2023b].

4.2.7. Subsidence

The initial compaction and oxidation of organic soils is included in the NUMAR model. Deep subsidence must be included separately when comparing modeled accretion to expected RSLR. The Louisiana Coastal Protection and Restoration Authority (CPRA) publishes shallow and deep subsidence rates for coastal Louisiana in their Master Plan [Fitzpatrick et al., 2021].

5. Calibrating and Validating Delta-X models

5.1. Hydrodynamic model

We used remote sensing and in situ data for calibration and validation of hydrodynamic and morphodynamic models for coastal wetlands in the Delta-X study area. Model parameters were refined based on the measured spatial and temporal distributions of water and sediment dynamics in these deltaic wetlands. The method was initially applied for broad scale, coarse resolution (90 m) regular mesh models of the Terrebonne and Atchafalaya study areas [Cortese et al., 2023; Cortese and Fagherazzi, 2023; Cortese et al., 2024] and a small scale, high resolution (10 m) regular mesh model of an intensive study site [Donatelli et al., 2023b]. These models were used to refine calibration methods for incorporation into the final Delta-X hydrodynamic and morphodynamic model based on Delft3D FM, described here [Payandeh et al., 2025a; Payandeh et al., 2025b; Payandeh et al., 2025c].

To capture seasonal variability in hydrological conditions, we ran the model for two 31-day periods in the fall and spring of 2021 coinciding with the Delta-X field campaigns. The first day of each simulation served as a warm up period and was excluded from all analyses. Model results for each season were then compared with remote sensing and in situ measurements to iteratively calibrate key hydrodynamic and sediment parameters. Fig. 15 shows the workflow for initializing, calibrating, and validating the Delft3D FM model. The steps taken were to 1) initiate the hydrodynamic portion of the model, 2) calibrate and validate the friction coefficients for both open water and vegetated areas, 3) initiate the morphodynamic model based on sediment field measurements, 4) calibrate and validate the morphodynamic transport parameters, then 5) simulate vertical inorganic accretion annual rates and 6) validate against accretion measurements from the CRMS stations. Each initiation, calibration, and validation step is described below.

Delft3D FM was implemented for the combined Atchafalaya and Terrebonne basin Delta-X study area using a flexible mesh (Fig. 16). Mesh generation was carried out in Aquaveo's Surface Water Modeling System (SMS) [Zundel, 2000]. A sensitivity analysis showed a grid size of at least 30 m is required to resolve small scale connectivity in the domain (Fig. 4), therefore, in SMS mesh resolution was strategically varied to capture landscape and hydrodynamic complexity: the highest resolution (~25 m element size) was applied within channels, smaller bayous, and along levees for accurate representation and to preserve connectivity. Adaptive mesh design followed standard practice in unstructured grid modeling: regions with complex terrain (e.g., channel bends, levees) were assigned finer triangular elements, while open floodplain or bathymetrically smoother zones used coarser resolution. The final mesh comprised 774,734 nodes and 1,543,682 elements (Fig. 16). The Delta-X DEM (Section 4.2.6 [Christensen et al., 2023b]) was then interpolated into this mesh to define model topobathymetry. The mesh quality, smoothness, and orthogonality were carefully reviewed and met standard numerical criteria before proceeding to simulation. Hourly water level data from the NOAA station at Eugene Island (station ID: 8764314) were used at the southern boundary. Neumann boundary conditions were applied at the eastern and western boundaries. Spatially uniform hourly wind magnitude and direction were also applied to the model using the same NOAA station (station ID:

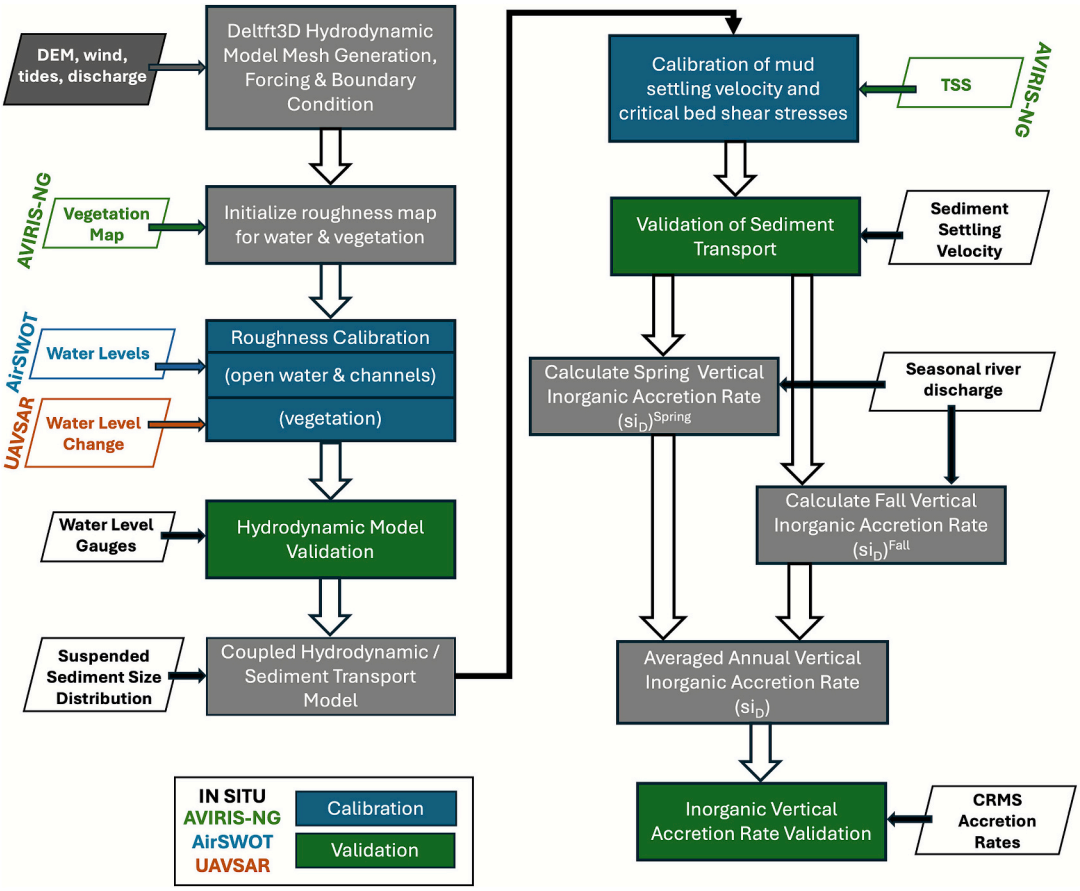

Fig. 15. The hydrodynamic and morphodynamic model calibration and validation within the Delta-X framework.

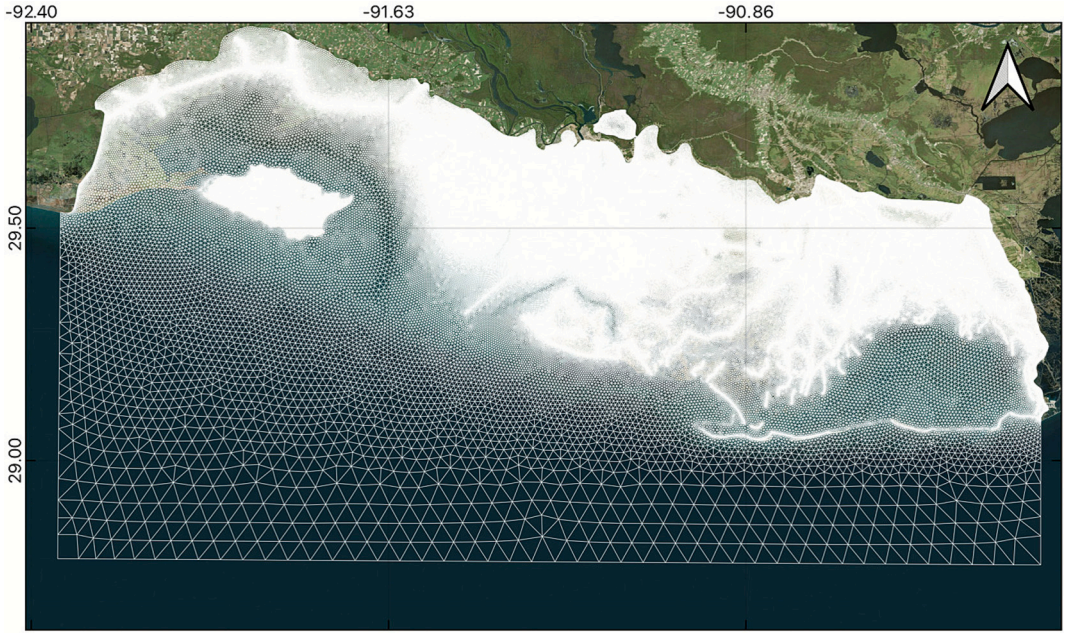

Fig. 16. Delft3D FM model domain and mesh.

8764314). To force river discharges in the model, data from the USGS stations in Calumet (station ID: 07381590) and Morgan City (station ID: 07381600) were used for the Wax Lake Outlet and Atchafalaya River boundaries respectively.

Friction coefficients were initiated based on a map of the vegetation classes. The vegetation map was initially developed using AVIRIS-NG data [Jensen et al., 2024a] and subsequently extended to cover the entire model domain using Sentinel-2 imagery. This is an example of

how satellite data can augment and gap-fill airborne remote sensing measurements within the Delta-X framework, primarily for vegetation where temporal repeat and overlap is not critical. Based on this map, we created a spatially variable Chézy roughness map by assigning initial distinct Chézy coefficients to each vegetation type. The initial Chézy coefficient maps were based on prior research conducted in the area [e.g., Xing et al., 2017; Cortese et al., 2024] and were refined through an iterative calibration process in which modeled water levels and water level changes were compared to AirSWOT and UAVSAR observations to improve initial guesses for the friction coefficients in the channels and wetland topography [Zhang et al., 2022a]. Modeled water levels were first compared with AirSWOT observations to calibrate roughness values for open water and channels. Then, water level changes from the model were compared with UAVSAR measurements to refine the Chézy coefficients assigned to different wetland vegetation types. Final validation of the hydrodynamic portion of the model was performed using in situ water level observations from Delta-X tide gauges. Table 5 shows the final Chézy coefficients assigned to each land cover type.

In the hydrodynamic model calibration process (Fig. 15), comparison between AirSWOT-measured and modeled water levels indicated that assigning a Chézy coefficient of 65 $m^{1/2}/s$ for open water and 60 $m^{1/2}/s$ for channels yielded the best agreement, improving RMSE in water-level predictions across the domain. When comparing all AirSWOT acquisitions with model, this calibration reduced RMSE from 18 cm to 9 cm for the spring simulation and from 14 cm to 10 cm for the fall simulation. AirSWOT's spatial data highlighted zones where the model underperformed, particularly in northern regions of the Terrebonne study area where the coarse grid resolution hindered accurate tidal propagation. Despite these challenges, calibration with AirSWOT water level data improved the model's ability to simulate water fluxes in bays, tidal channels, and distributaries. UAVSAR played a complementary role in calibrating the Chézy values assigned to different wetland vegetation types. Comparing modeled water level changes with UAVSAR data indicated that higher friction values should be assigned to soil/built areas, forests, broadleaf herbaceous, and reed/tall grass zones, while relatively lower friction is appropriate for freshwater grasses, saltmarsh grasses, and aquatic vegetation. The calibrated Chézy coefficients for these zones ranged from 30 to 57 $m^{½}\text{-}s^{-1}$ (Table 5). These values fall within the range of coefficients used in previous Delta-X studies (e.g., [Cortese et al., 2023; Castañeda-Moya and Solohin, 2023a, 2023b, 2023c, 2023d, 2023e]) that had coarser spatial resolutions and three broad categories of open sea/ocean, tidal channels/lakes/bays, and marsh platform [Castañeda-Moya and Solohin, 2023a, 2023b, 2023c, 2023d, 2023e; Cortese et al., 2023]. In contrast, the final implementation of our model was based on an updated vegetation map that defined nine distinct surface types. These included six vegetation classes (forests, broadleaf herbaceous, reed/tall grass, freshwater grasses, saltmarsh grasses, and aquatic vegetation) and three non-vegetated classes (soil/mudflat, channel/bayou, and open water).

The hydrodynamic model was validated by comparing its outputs with water level observations from Delta-X tide gauges [Christensen et al., 2023a]. Overall, the results showed a strong agreement between simulated and observed water levels across all gauges, with R^2 of 0.86 for the spring simulation and 0.60 for the fall. The reduced correlation in fall is likely due to greater impacts from localized wind patterns and storm events, which can introduce variability not captured by the use of spatially uniform wind inputs [Sorourian et al., 2020]. The RMSE was 0.09 m for the spring period and 0.11 m for the fall.

Table 5
Final calibrated Chézy coefficients assigned to each land cover type.

Land cover type	Chézy coefficient ($m^1/^2/s$)
soils/built	30
forest	32
broadleaf herbaceous	35
reed/tall grass	40
freshwater grass	45
saltmarsh grass/brackish grass	50
aquatic vegetation	57
channels/bayous	60
open water	65

For the morphodynamic model calibration (Fig. 15), AVIRIS-NG provided maps of TSS that were critical for inferring spatial patterns of suspended sediment used to calibrate sediment transport parameters, specifically the settling velocity and critical shear stresses for erosion and deposition [Salter et al., 2022]. For morphodynamic model calibration, modeled suspended sediment concentrations were compared against AVIRIS-NG-derived total suspended solid concentration [Fichot and Harringmeyer, 2023a], focusing on tuning the mud settling velocity and the critical bed shear stresses for erosion and deposition. The best agreement between modeled and observed sediment concentrations was achieved with a settling velocity of 0.1 mm/s and critical shear stresses for erosion of 0.5 Pa and for deposition of 0.1 Pa. The final calibrated values are consistent with in situ settling velocity measurements that ranged from 0.1 to 1 mm/s [Nghiem et al., 2024].

After calibration and validation, we used the coupled hydrodynamic and morphodynamic models to calculate inorganic mass accretion rates (si_D) for both fall and spring. To derive annual rates, we combined the seasonal results using a weighted average based on the probability density function (PDF) of historical Atchafalaya River discharge. Discharge data from USGS station in Morgan City (station id: 07381600) was used to calculate the weighting coefficients. The weighting coefficients were calculated by dividing the PDF of the mean discharge for each simulation period by the sum of the PDFs for both periods. This approach assigns greater weight to conditions that occur more frequently, with the fall (low discharge) simulation weighted at 0.72 and the spring (high discharge) simulation weighted at 0.28, providing a discharge-representative annual estimate.

To assess the accuracy and uncertainty of model, we compared the weighted averaged si_D from Delft3D FM with accretion measurements made at the CRMS stations within the study domain. Fig. 17 shows a scatter plot of modeled versus observed si_D, showing an R^2 of 0.61, a mean absolute error (MAE) of 0.13 $g{\cdot}cm^{-2}{\cdot}yr^{-1}$ and a bias of −0.10 $g{\cdot}cm^{-2}{\cdot}yr^{-1}$, indicating a modest underestimation by the model. The bias was calculated as the mean of the residuals (model predictions minus observed CRMS rates), and the MAE is the average of the absolute values of those residuals. A key challenge in this validation is the limited availability and inherent uncertainty of CRMS accretion data. Accretion rates at a single station can vary substantially over time and between replicate measurements. Moreover, feldspar marker horizons used at CRMS stations only record positive accretion because erosional events remove the marker completely, so they inherently overestimate net sediment accumulation. By contrast, our model captures both deposition and erosion. These measurement limitations have been noted in previous studies (e.g., [Bianchette et al., 2015; Bansal et al., 2023]) and highlight the difficulty of benchmarking morphodynamic models against field-based estimates.

Overall, the coupling of remote sensing data with numerical models provided substantial improvements in spatial accuracy compared to traditional in situ methods, which are limited to point measurements and lack spatial variability. The integration of UAVSAR, AirSWOT, and AVIRIS-NG enabled identification of critical areas where models performed poorly, site-specific parameter calibration, and model results capable of capturing both hydrodynamic and morphodynamic with improved accuracy. All of this demonstrates the value of the Delta-X framework's leveraging remote sensing data to develop calibrated, spatially comprehensive numerical models for coastal wetland systems.

5.2. Landscape ecogeomorphic model

The NUMAR model described in Section 3.4.2 and available online [Twilley et al., 2024c, 2024d] can be applied to a specific site, multiple

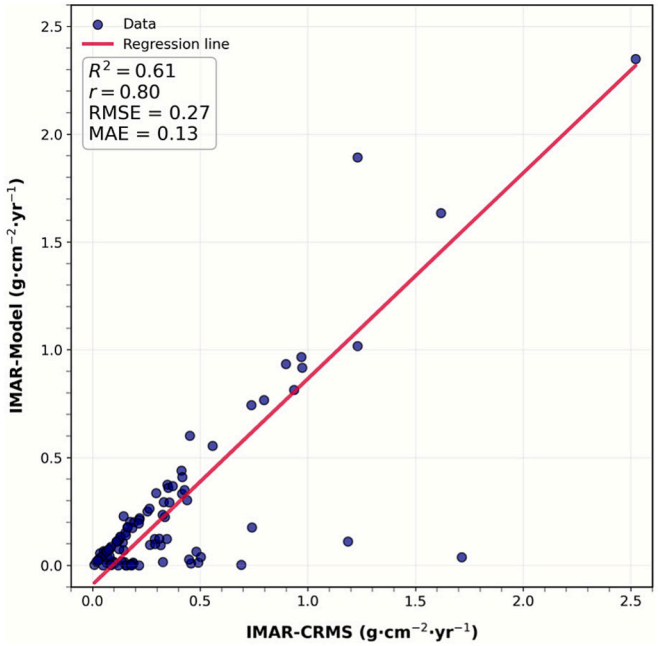

Fig. 17. Comparison of modeled and observed si_D from accretion measurements at the CRMS stations within the study area.

sites, or across gridded surface landscapes to produce maps of long-term (i.e., multi-decadal) soil development through surface and subsurface processes. The model is parameterized with fifteen variables, each of which were determined through field measurements and calibration over the six Delta-X intensive sites [Fontenot, 2022; Twilley et al., 2024a, 2024b]. The long-term soil accretion rate for the multiple intensive study sites was tested by hindcasting and comparing to long-term soil accretion rates determined from ^{137}Cs soil profile dating [Twilley et al., 2024a]. This technique is based on detecting peak ^{137}Cs activity in a soil profile that corresponds to the radionuclide fallout of cesium in 1963 during atmospheric nuclear testing. This peak provides a temporal reference for determining long term sediment deposition and marsh accretion rates [Ritchie and McHenry, 1990; Walling and He, 1997].

To scale the NUMAR model to the full Delta-X domain, we classified the landscape into seven landcover types: forest, and active fresh, active brackish, active saline, inactive fresh, inactive brackish, and inactive saline herbaceous wetlands. With the exception of forest type, these correspond to the intensive study sites where NUMAR model calibration data were collected (Sections 4.2.1 and 4.2.2). Assignment of these classes across the landscape was determined using a combination of the Delta-X Vegetation Type maps (Jensen et al., 2024a) for identifying whether the area was fresh, brackish, or saline, and a map of active and inactive resgions. We improved upong a previous map (Twilley et al., 2019a, 2019b) using two sets of Delft3D FM simulations to establish the region exposed to riverine sediment. The simulations were conducted for the fall and spring periods: one with river discharge included and with river discharge turned off. The additional sediment accumulation in the simulations with river discharge highlights regions receiving sediments from rivers, i.e., the active areas. Finally, the results from the two seasons were combined to identify active versus inactive regions representative of the entire year. Six of the nine model input parameters (bo, bi, c2, c4, kc, and kl) were determined to be constant for all field sites and applied uniformly to all landcover types. Seven of the nine model input parameters (oms, c0, c1, e, fc1, kb, kr) were applied to each landcover class based on results from Twilley et al. [2024d]. The NUMAR model is designed for simulating soil development in herbaceous marshes. In the absence of a forest intensive study site, values for that class were assigned using input parameters derived from mangrove sites from Shribman [2021] (r0 and e), freshwater active herbaceous sites from Fontenot [2022] (kb) and Delta-X field data (oms), and the mangrove NUMAN model by Biswas et al. [2025] (b0, b1, c0, c2, c4, fc1, kc, kl, kr).

The remaining two input parameters for the landscape model (r0 and si) were determined using output from other Delta-X products. The live root biomass at the surface, r0, was determined using maps of belowground biomass from AVIRIS-NG (Jensen et al., 2025d), derived from a combination the AVIRIS-NG herbaceous aboveground biomass products and field data [Castañeda-Moya and Solohin, 2022; Jensen et al., 2024b; Jensen et al., 2025a], with simple attenuation (using parameter e) to convert total to surface root biomass (r0). AVIRIS-NG belowground biomass data were not available in forested areas and were instead estimated from Shribman [2021]. Delft3D's weighted average vertical inorganic accretion rate, si_D, was used for the NUMAR model parameter si, the inorganic matter loading rate (see Section 5.3).

5.3. *Coupling of the hydrodynamic model with the landscape Ecogeomorphic model*

At its basic level, the hydrodynamic model and the ecogeomorphic model are coupled through the use of Delft3D FM's modeled output for the vertical inorganic accretion rate, si_D, in the landscape ecogeomorphic model. In its simplest implementation, the NUMAR model can be run for many years (79 in our case to estimate land loss or gain by the year 2100) using the one annual estimate of si_D based on the data collected in the spring and fall Delta-X campaigns. However, more advanced couplings can be applied subject to the constraint that NUMAR is not intended to model yearly accretion, but rather values averaged over many years, 10 or more. One could add coupling complexity by iteration between the two models, e.g., 1) calculating si_D in Delft3D FM, 2) using NUMAR to predict the combined inorganic and organic accretion over some time period, e.g., 10, 20, or more years, 3) updating the DEM in the Delft3D FM hydrodynamic and morphodynamic model based on total accretion over that time period, 4) rerunning Delft3D FM to determining si_D for the next time period, and so on until reaching the desired end date. The next level of complexity would be to update the vegetation class map (e.g., [Glick et al., 2013]) in addition to the DEM at the end of each iteration. However, this added complexity may introduce additional uncertainty related to our understanding of species transition processes. For this reason, either the single estimate or iteratively changing the DEM is recommended unless there is very good knowledge of vegetation growth and turnover rates at the particular site under study.

Equally important for using the model to forecast future conditions is estimating the uncertainty in the modeled future topobathymetric map. For the Delta-X study site, NUMAR results of long-term accretion are most sensitive to the belowground biomass, r0, the modeled inorganic accretion rate, siD, and decomposition, kr, although other studies implementing the Delta-X framework should do a one-variable-at-a-time statistical analysis to determine their most sensitive parameters in the coupled model. As reported in Section 5.1, for our study site the MAE of si_D, as compared with CRMS measurements of si, is 0.13 g/cm^2/yr, and the MAE of belowground biomass from AVIRIS-NG is 490 g/m^2, resulting in r0 errors of 0.0001–0.0007 g/cm^2, depending on the landcover class. For general implementation of the framework, typical error analysis involves varying the most significant parameters across their range of likely values and running the models to get new limiting estimates. A Monte Carlo method varying some or all parameters within their likely ranges is also an option, but may be computationally impractical depending upon the domain size (as is the case for Delta-X).

It is difficult to assess the long-term accuracy of our approach since the NUMAR model predicts soil accretion after 79 years (2021−2100) of surface and subsurface physical and biological dynamics. An accuracy assessment of NUMAR's hindcasting capability using ^{137}Cs at the six intensive field sites is presented in Fig. 6 of Twilley et al. [2024a]. Long

term predications rely on well-calibrated models, which the Delta-X framework provides. As described previously, each model is validated after each calibration step, so they are well set up to use for long-term predictions. Limitations of note and possible changes to address them are described below.

5.4. Limitations

Inevitably, modeling a system with the complexity of a delta has limitations. Here, we document the most important challenges and limitations encountered with the airborne and in situ observations and the hydrodynamic, morphodynamic and ecogeomorphic models, and their coupling.

The most significant limitation to the observational component was in selection of the number and location of the extensive study sites because that fed directly into the calibration of the NUMAR model, the complexity and realism of classification in the landscape NUMAR model, and calibration of the AVIRIS-NG data. This component of field work requires a compromise between time and budget. Similarly, the field measurements of accretion rates are made at a limited number of sites (in our case both the intensive study sites and CRMS stations throughout the study domain), and those sites can be abnormally impacted by storms making them not representative of the entire landscape. ^{137}Cs validation measurements are similarly limited. For Delta-X, belowground biomass estimates using AVIRIS-NG were challenged by limited field measurements, and particularly stormy weather in the study area introduced imaging and atmospheric artifacts into the radar data [Belhadj-aissa et al., 2024; Oliver-Cabrera et al., 2025].

In addition, the topobathymetric DEM is critical to realistic hydrodynamic modeling and, as spelled out in Section 4.2.6, we used the most accurate data available. Observation of channel-island connectivity is of particular importance to determining whether the input bathymetry map is realistic, particularly in areas with low relief. Although not implemented for the full domain because of incomplete coverage due to atmospheric artifacts, UAVSAR measurements of water-level changes were used to improve marsh topography by iteratively comparing the modeled and observed water-level changes for a small part of the study area in the Atchafalaya basin [Zhang et al., 2022a], proving InSAR's potential for improving DEMs in wetlands. Initial simulations revealed discrepancies, particularly a latitudinal bias in the small-scale model, where water level changes were overestimated in the south and underestimated in the north. Iterative adjustments to marsh elevation reduced the root mean square error (RMSE) in water-level change from 18.9 cm to 9.8 cm in the small-scale model [Zhang et al., 2022b; Cortese et al., 2024]. This correction highlighted the importance of accurate marsh topography, particularly in low tidal range environments like coastal Louisiana where small elevation changes significantly affect flooding dynamics. By incorporating UAVSAR data, the model captured local micro-topographic variations that were missed by the lidar-derived DEM, which is prone to vegetation-related biases.

The NUMAR model is designed for simulating soil development in herbaceous marshes. However, in the current NUMAR implementation, we simulate soil development in forests using input parameters from mangrove sites. This represents a significant limitation in our current implementation as mangroves and bottomland hardwood forests, a common forest type in the Atchafalaya basin, have different ecosystem structure and function. More field measurements in these forests would be needed to better parameterize the NUMAR model in these areas. Forest aboveground biomass maps [Jensen et al., 2025b] were derived from the combination of AVIRIS-NG and UAVSAR data following Jensen et al. [2019a] and belowground biomass could be estimated from these maps based on published root:shoot ratios for the dominant tree species.

Another limitation of the NUMAR model is the fixed parameterization for all years in the simulation despite the fact that as the model progresses, parameters such as si, r0, and other soil parameters may change, especially as elevation increases, the marsh migrates, and vegetation type evolves eg. [Rovai et al., 2022; Cahoon et al., 2021]. Indeed, given the spatial distribution of the six classes (i.e. active saline, brackish and fresh and inactive saline, brackish and fresh) across the landscape may change in the future, particularly between the saline versus brackish classes as the topography and sea level changes. Moreover, changes in vegetation cover will impact the hydrodynamic model through the assignment of Chézy roughness values.

The numerical hydrodynamic model has inherent limitations related to spatial resolution. Delta-X final mesh, with a minimum resolution of 25 m, provides reasonably detailed representation of small-scale geographic features in the study area. However, many natural and manmade channels, as well as fine-scale topobathymetric features that are smaller than 25 m, were likely not resolved. Previous Delta-X studies in intensive sites applying a 10 m model showed that small-scale topographic features can significantly control spatial variability in drainage patterns within vegetated areas [Donatelli et al., 2023c]. This highlights the need for caution when interpreting model outputs in areas where sub-25 m features may play a significant hydrodynamic role. Despite this, 25 m was the finest resolution feasible at the study scale under existing computational constraints. Furthermore, spatially uniform hourly wind magnitude and direction were applied to the model, neglecting the spatial variability of wind fields that can significantly influence hydrodynamic processes in the Delta-X large domain. Incorporating spatially varying wind forcing has been shown to improve model accuracy, particularly in systems with complex shoreline geometry and heterogeneous exposure to wind fetch [e.g., Mariotti et al., 2018; Valentine and Mariotti, 2019].

Finally, the accretion rates from the fall and spring simulations were weighted averaged to obtain annual rates. These weighting coefficients were based on the river discharges in 2021. However, historical data from 1996 to 2024 indicate that the number of days per year with discharges exceeding the long-term mean has increased (Figure S-2). Consequently, future decadal trends in river discharge could influence sediment concentrations, potentially introducing uncertainty into long-term predictions. These unknowns are best accounted by modeling the uncertainties as described in Section 5.3. Finally, because of the computational load, our model does not include waves, which could alter the results. It is recommended that waves be included, if possible, when implementing the framework.

6. Conclusions

Coastal wetlands are hydrodynamically complex environments: A dendritic network of creeks dissects the marsh platform; man-made channels are often dug within the network; and it can be difficult to determine whether any specific channel, particularly small ones, convey water or are inactive. Additionally, the marsh platform exchanges water with the channels during some but not all conditions, an exchange that is driven by subtle differences in water level and by the slope of the water surface. As a result, the influence of flow into adjacent wetlands on channelized discharge varies in both space and time. Instruments deployed in the field can seldom capture these complex flows. Even to characterize the fluxes of water and sediments in a small part of the delta requires hundreds of tidal gauges and flow meters to instrument all channels.

The Delta-X framework presented here is designed to address the challenge through a combination of airborne remote sensing, field campaigns, and modeling. Importantly, the framework is applicable to any delta, although the details of the implementation should vary depending upon the specifics of the environment. The methodology is sufficiently general to be tailored to other landscapes, ecosystems, and hydrological regimes. High resolution spatial data derived from currently available airborne sensors provide important information on the functioning of coastal wetland systems. Their spatially extensive measurements provide new insight into flows and mass balance that can be used to calibrate and validate hydrodynamic, morphodynamic, and

organic productivity models that in combination model the wetland environment at the hectare scale. The framework specifies the remote sensing and in situ measurements needed to develop, calibrate, and validate a combined hydraulic, morphodynamic, and land-evolution model in concert with an ecogeomorphic numerical soil accretion model that tracks organic productivity. It requires rapid repeat imaging, currently only possible with an airborne campaign, for observing hydrological processes in a deltaic setting where tides propagate across the landscape, changing water surface slopes and creating overflows to the wetlands.

The Delta-X framework was implemented successfully for the Mississippi River Delta for two adjacent areas, one undergoing significant land gain (Atchafalaya) and the other significant land loss (Terrebonne), and the study area extent was limited by manmade levees that artificially cut off connectivity. This implementation is described in detail herein to facilitate adoption of the framework in other coastal areas. For the Delta-X mission, data were collected in spring and fall campaigns to cover the range of river discharge, sediment supply, and vegetation conditions in the MRD. Collections were made during high spring floods when much of the vegetation starts to resprout, then later in the same year when discharge was reduced and vegetation had reached its peak biomass. Other sites' tidal range, topographic relief, discharge conditions, vegetation phenology, and anthropogenic modifications will modify coverage and timing of the remote sensing measurements. However, the types of information collected within the Delta-X framework and how it is used to forecast elevation change in coastal wetlands at the hectare scale remains relevant.

The Delta-X mission made extensive use of NASA airborne assets (UAVSAR, AirSWOT and AVIRIS-NG) and sets the stage for three new or proposed NASA spaceborne missions which have similar capabilities: Surface Water and Ocean Topography (SWOT, launched in December 2022), NASA-ISRO Synthetic Aperture Radar (NISAR, launched in July 2025), and Surface Biology and Geology (SBG) [NAS, 2019]. The extent to which the Delta-X framework presented here and implemented for the Mississippi River Delta can be simplified or complemented by incorporating data from satellite sensors remains a topic for study as more and better data covering deltas becomes available. Airborne remote sensing instruments are currently the only source of observations with a cadence sufficient to track tidal propagation.

CRediT authorship contribution statement

Marc Simard: Writing – review & editing, Writing – original draft, Validation, Supervision, Project administration, Methodology, Investigation, Funding acquisition, Formal analysis, Conceptualization. **Cathleen E. Jones:** Writing – review & editing, Writing – original draft, Validation, Supervision, Software, Project administration, Methodology, Investigation, Funding acquisition, Formal analysis, Conceptualization. **Robert R. Twilley:** Writing – review & editing, Writing – original draft, Supervision, Methodology, Investigation, Funding acquisition, Formal analysis, Conceptualization. **Edward Castañeda-Moya:** Writing – review & editing, Writing – original draft, Validation, Supervision, Methodology, Investigation, Funding acquisition, Formal analysis, Data curation, Conceptualization. **Sergio Fagherazzi:** Writing – review & editing, Writing – original draft, Validation, Supervision, Methodology, Investigation, Funding acquisition, Formal analysis, Conceptualization. **Cédric G. Fichot:** Writing – review & editing, Writing – original draft, Validation, Supervision, Methodology, Investigation, Funding acquisition, Formal analysis, Conceptualization. **Michael P. Lamb:** Writing – review & editing, Writing – original draft, Supervision, Methodology, Investigation, Funding acquisition, Formal analysis, Conceptualization. **Paola Passalacqua:** Writing – review & editing, Writing – original draft, Supervision, Methodology, Investigation, Funding acquisition, Formal analysis, Conceptualization. **Tamlin M. Pavelsky:** Writing – review & editing, Writing – original draft, Validation, Supervision, Methodology, Investigation, Funding acquisition, Formal analysis, Conceptualization. **David R. Thompson:** Writing – original draft, Visualization, Supervision, Methodology, Funding acquisition, Formal analysis, Data curation, Conceptualization. **Saoussen Belhadj-aissa:** Writing – review & editing, Software, Formal analysis. **Pradipta Biswas:** Writing – review & editing, Software, Formal analysis, Data curation. **Alexandra Christensen:** Writing – review & editing, Visualization, Software, Investigation, Formal analysis, Data curation. **Luca Cortese:** Writing – review & editing, Validation, Software, Investigation, Formal analysis. **Michael Denbina:** Writing – review & editing, Validation, Software, Methodology, Formal analysis, Data curation. **Carmine Donatelli:** Validation, Software, Investigation, Formal analysis. **Sarah Flores:** Writing – review & editing, Visualization, Software, Data curation. **Andy Fontenot:** Writing – review & editing, Validation, Methodology, Investigation, Formal analysis. **Joshua P. Harringmeyer:** Writing – review & editing, Validation, Methodology, Investigation, Formal analysis, Data curation. **Daniel Jensen:** Writing – review & editing, Visualization, Validation, Methodology, Formal analysis, Data curation. **John Mallard:** Validation. **Justin Nghiem:** Writing – review & editing, Validation, Methodology, Formal analysis, Data curation. **Talib Oliver-Cabrera:** Writing – review & editing, Visualization, Software, Methodology, Formal analysis, Data curation. **Ali Reza Payandeh:** Writing – review & editing, Writing – original draft, Software, Investigation, Formal analysis. **Andre S. Rovai:** Writing – review & editing, Supervision, Methodology, Formal analysis, Data curation. **Elena Solohin:** Writing – review & editing, Validation, Formal analysis, Data curation. **Antoine Soloy:** Writing – review & editing, Methodology, Formal analysis. **Bhuvan Varugu:** Writing – review & editing, Methodology, Formal analysis, Data curation. **Dongchen Wang:** Writing – review & editing, Software, Methodology, Formal analysis. **Kyle Wright:** Writing – review & editing, Visualization, Software, Methodology, Investigation, Formal analysis. **Xiaohe Zhang:** Writing – review & editing, Visualization, Validation, Software, Methodology, Investigation, Formal analysis. **Yang Zheng:** Writing – review & editing, Supervision, Project administration, Funding acquisition.

Declaration of competing interest

The authors declare that they have no known competing financial interests or personal relationships that could have appeared to influence the work reported in this paper.

Acknowledgments

This work was carried out in part at the Jet Propulsion Laboratory, California Institute of Technology, under contract with the National Aeronautics and Space Administration (80NM0018D0004). The NASA Delta-X project is funded by the Science Mission Directorate's Earth Science Division through the Earth Venture Suborbital-3 Program NNH17ZDA001N-EVS3. JN, JH, and LC were partially supported by NASA FINESST grants 80NSSC20K1645 (PI MPL) and 80NSSC20K1648 (PI CGF) and 80NSSC21K1612 (PI SF), respectively. We thank Gerard Salter for initial development of the bed-material load model and upscaling framework, and Gerard Salter and Gen Li for help with sediment transport measurements. We thank Matthew Weiser, Hope Vanderhider, Nilotpal Ghosh, and Xiaohui Zhu for help with in situ sampling and/or processing of samples in the laboratory. We also thank Paul Miller of Louisiana State University for providing detailed weather forecasts and guidance during the campaigns. We acknowledge the participation of the late William "Bill" Gibson who conducted field measurements during the Spring campaign 2021. We recognize the support of previous Delta-X managers, Ian McCubbin and Judy Lai-Norling, who supported the formulation and execution of the campaigns.We are grateful to all Delta-X team members and the airborne instrument and flight crews, without whom the mission would not have been successful. This is contribution number 2093 from the Institute of Environment at Florida International University.

Appendix A. Supplementary data

Supplementary data to this article can be found online at https://doi.org/10.1016/j.rse.2025.115201.

Data availability

The datasets from the in situ campaigns and the airborne campaigns, and all derived information, models, and model output for Delta-X are archived by the Oak Ridge National Laboratory (ORNL) Distributed Active Archive Center (DAAC) [https://daac.ornl.gov/get_data/].

References

Bansal, S., Creed, I.F., Tangen, B.A., Bridgham, S.D., Desai, A.R., Krauss, K.W., Neubauer, S.C., Noe, G.B., Rosenberry, D.O., Trettin, C., Wickland, K.P., 2023. Practical guide to measuring wetland carbon pools and fluxes. Wetlands 43 (8), 105.

Belhadj-aissa, S., Simard, M., Jones, C.E., Oliver-Cabrera, T., Christensen, A., 2024. Separation of water level change from atmospheric artifacts through application of independent component analysis to InSAR time series. Earth and Space Science 11 (7), e2024EA003540.

Bevington, A.E., Twilley, R.R., 2018. Island edge morphodynamics along a chronosequence in a prograding deltaic floodplain wetland. J. Coast. Res. 34 (4), 806–817.

Bevington, A.E., Twilley, R., Sasser, C.E., 2022. Deltaic floodplain wetland vegetation dynamics along the sediment surface elevation gradient and in response to disturbance from river flooding and hurricanes in wax Lake Delta, Louisiana, USA. Geomorphology 398, 108011.

Payandeh, A.R., Justic, D., Huang, H., Mariotti, G., Hagen, S.C., 2022. Tidal change in response to the relative sea level rise and marsh accretion in a tidally choked estuary. Contin. Shelf Res. 234, 104642.

Bianchette, T.A., Liu, K.B., Qiang, Y., Lam, N.S.N., 2015. Wetland accretion rates along coastal Louisiana: spatial and temporal variability in light of Hurricane Isaac's impacts. Water 8 (1), 1.

Biswas, P., 2024. Developing the next generation of models for predicting soil formation in mangrove (NUMAN 2.0) and marsh (NUMAR 2.0) wetlands. Master's thesis. Louisiana State University. https://repository.lsu.edu/gradschool_theses/6008/.

Biswas, P., Twilley, R.R., Rovai, A.S., Christensen, A., Shribman, Z.I., Kameshwar, S., 2025. Incorporating uncertainty in a wetland soil accretion model (NUMAN 2.0) to test generality across coastal environmental settings of South Florida. Estuar. Coast. Shelf Sci. 323, 109407.

Byrd, K.B., O'Connell, J.L., Di Tommaso, S., Kelly, M., 2014. Evaluation of sensor types and environmental controls on mapping biomass of coastal marsh emergent vegetation. Remote Sens. Environ. 149, 166–180.

Cahoon, D.R., Turner, R.E., 1989. Accretion and canal impacts in a rapidly subsiding wetland II. Feldspar marker horizon technique. Estuaries 12, 260–268.

Cahoon, Donald R., McKee, Karen L., Morris, James T., 2021. How plants influence resilience of salt marsh and mangrove wetlands to sea-level rise. Estuar. Coasts 44 (4), 883–898.

Callaway, J.C., Nyman, J.A., DeLaune, R.D., 1996. Sediment accretion in coastal wetlands: a review and a simulation model of processes. Curr. Top. Wetland Biogeochemi. 2 (2), 23.

Carle, M.V., Sasser, C.E., Roberts, H.H., 2015. Accretion and vegetation community change in the wax Lake Delta following the historic 2011 Mississippi River flood. J. Coast. Res. 31 (3), 569–587.

Cassaway, A.F., Twilley, R.R., Rovai, A.S., Snedden, G.A., 2024. Patterns of marsh surface accretion rates along salinity and hydroperiod gradients between active and inactive coastal deltaic floodplains. Estuar. Coast. Shelf Sci. 301, 108757.

Castañeda-Moya, E., Solohin, E., 2022. Delta-X: belowground biomass and Necromass across wetlands, MRD, LA, USA, 2021, V2. ORNL DAAC, Oak Ridge, Tennessee, USA. https://doi.org/10.3334/ORNLDAAC/2238.

Castañeda-Moya, E., Solohin, E., 2023a. Delta-X: aboveground vegetation structure, herbaceous wetlands, MRD, LA, USA, V2. ORNL DAAC, Oak Ridge, Tennessee, USA. https://doi.org/10.3334/ORNLDAAC/2240.

Castañeda-Moya, E., Solohin, E., 2023b. Delta-X: aboveground biomass and Necromass across wetlands, MRD, Louisiana, 2021, V2. ORNL DAAC, Oak Ridge, Tennessee, USA. https://doi.org/10.3334/ORNLDAAC/2237.

Castañeda-Moya, E., Solohin, E., 2023c. Delta-X: Foliar Stable Isotopes, MRD, LA, USA, 2021. ORNL DAAC, Oak Ridge, Tennessee, USA. https://doi.org/10.3334/ORNLDAAC/2194.

Castañeda-Moya, E., Solohin, E., 2023d. Delta-X: root stable isotopes from herbaceous wetlands, MRD, LA, USA, august 2021. ORNL DAAC, Oak Ridge, Tennessee, USA. https://doi.org/10.3334/ORNLDAAC/2193.

Castañeda-Moya, E., Solohin, E., 2023e. Delta-X: soil properties for herbaceous wetlands, MRD, Louisiana, 2021, V3. ORNL DAAC, Oak Ridge, Tennessee, USA. https://doi.org/10.3334/ORNLDAAC/2239.

Chapman, J.W., Thompson, D.R., Helmlinger, M.C., Bue, B.D., Green, R.O., Eastwood, M. L., Lundeen, S.R., 2019. Spectral and radiometric calibration of the next generation airborne visible infrared spectrometer (AVIRIS-NG). Remote Sens. 11 (18), 2129.

Chen, R., Twilley, R.R., 1999. A simulation model of organic matter and nutrient accumulation in mangrove wetland soils. Biogeochemistry 44, 93–118.

Christensen, A., Twilley, R.R., Willson, C.S., Castañeda-Moya, E., 2020. Simulating hydrological connectivity and water age within a coastal deltaic floodplain of the Mississippi River Delta. Estuar. Coast. Shelf Sci. 245, 106995.

Christensen, A.L., Mallard, J.M., Nghiem, J., Simard, M., Pavelsky, T.M., Lamb, M.P., 2022a. Delta-X: acoustic Doppler current Profiler Channel surveys, MRD, Louisiana, 2021, V2. ORNL DAAC, Oak Ridge, Tennessee, USA. https://doi.org/10.3334/ORNLDAAC/2081.

Christensen, A.L., Mallard, J.M., Nghiem, J., Harringmeyer, J., Simard, M., Pavelsky, T. M., Lamb, M.P., Fichot, C.G., 2022b. Delta-X: sonar bathymetry survey of channels, MRD, Louisiana, 2021. ORNL DAAC, Oak Ridge, Tennessee, USA. https://doi.org/10.3334/ORNLDAAC/2085.

Christensen, A.L., Mallard, J.M., Simard, M., Pavelsky, T.M., Rovai, A., 2023a. Delta-X: in-situ water surface elevation, MRD, Louisiana, USA, 2021. ORNL DAAC, Oak Ridge, Tennessee, USA. https://doi.org/10.3334/ORNLDAAC/2086.

Christensen, A.L., Denbina, M.W., Simard, M., 2023b. Delta-X: Digital Elevation Model, MRD, LA, USA, 2021. ORNL DAAC, Oak Ridge, Tennessee, USA. https://doi.org/10.3334/ORNLDAAC/2181.

Coastal Protection and Restoration Authority (CPRA) of Louisiana, 2023. Coastwide Reference Monitoring System-Wetlands Monitoring Data. Retrieved from Coastal Information Management System (CIMS) database. http://cims.coastal.louisiana.gov. Accessed 01 December 2024.

Cortese, L., Fagherazzi, S., 2023. Delta-X: Delft3D Broad-Scale Sediment Model, Terrebonne Basin, MRD, Louisiana, USA. ORNL DAAC, Oak Ridge, Tennessee, USA. https://doi.org/10.3334/ORNLDAAC/2301.

Cortese, L., Zhang, X., Fagherazzi, S., 2023. Delta-X: Delft3D Broad-Scale Sediment Model, Atchafalaya Basin, MRD, Louisiana, USA. ORNL DAAC, Oak Ridge, Tennessee, USA. https://doi.org/10.3334/ORNLDAAC/2302.

Cortese, L., Donatelli, C., Zhang, X., Nghiem, J.A., Simard, M., Jones, C.E., Fagherazzi, S., 2024. Coupling numerical models of deltaic wetlands with AirSWOT, UAVSAR, and AVIRIS-NG remote sensing data. Biogeosciences 21, 241–260. https://doi.org/10.5194/bg-21-241-2024.

Couvillion, B.R., Barras, J.A., Steyer, G.D., Sleavin, W., Fischer, M., Beck, H., Heckman, D., 2011. Land area change in coastal Louisiana from 1932 to 2010. U.S. Geological Survey Scientific Investigations Map 3164, p. 12 scale 1:265,000.

Day Jr., J.W., Rybczyk, J., Scarton, F., Rismondo, A., Are, D., Cecconi, G., 1999. Soil accretionary dynamics, sea-level rise and the survival of wetlands in Venice lagoon: a field and modelling approach. Estuar. Coast. Shelf Sci. 49 (5), 607–628.

De Leeuw, J., Lamb, M.P., Parker, G., Moodie, A.J., Haught, D., Venditti, J.G., Nittrouer, J.A., 2020. Entrainment and suspension of sand and gravel. Earth Surf. Dyn. 8 (2), 485–504. https://doi.org/10.5194/esurf-8-485-2020.

Deltares, 2021a. Delft3D FM Suite; D-flow Manual. Technical Report. Deltares. Version as of 2021a.

Deltares, 2021b. Delft3D FM Suite; D-morphology Manual. Technical Report. Deltares. Version as of 2021b.

Denbina, M., Simard, M., Rodriguez, E., Wu, X., Chen, A., Pavelsky, T., 2019. Mapping water surface elevation and slope in the Mississippi River Delta using the AirSWOT Ka-band interferometric synthetic aperture radar. Remote Sens. 11 (23), 2739.

Denbina, M.W., Simard, M., Pavelsky, T.M., Christensen, A.I., Liu, K., Lyon, C., 2020. Pre-Delta-X: channel bathymetry of the Atchafalaya Basin, LA, USA, 2016. ORNL DAAC, Oak Ridge, Tennessee, USA. https://doi.org/10.3334/ORNLDAAC/1807.

Denbina, M.W., Simard, M., Rodriguez, E., 2021. Delta-X: AirSWOT level 1B Interferogram products in radar coordinates, 2021. ORNL DAAC, Oak Ridge, Tennessee, USA. https://doi.org/10.3334/ORNLDAAC/1996.

Denbina, M.W., Simard, M., Rodriguez, E., 2022. Delta-X: AirSWOT L3 water surface elevations, MRD, Louisiana, 2021. ORNL DAAC, Oak Ridge, Tennessee, USA. https://doi.org/10.3334/ORNLDAAC/2133.

Denbina, M.W., Simard, M., Rodriguez, E., 2023. Delta-X: AirSWOT L2 geocoded water surface elevation, MRD, Louisiana, 2021, version 2. ORNL DAAC, Oak Ridge, Tennessee, USA. https://doi.org/10.3334/ORNLDAAC/2128.

Deverel, S.J., Dore, S., Schmutte, C., 2020. Solutions for subsidence in the California Delta, USA, an extreme example of organic-soil drainage gone awry. Proceedings of the International Association of Hydrological Sciences 382, 837–842.

Donatelli, C., Passalacqua, P., Wright, K., Salter, G., Lamb, M.P., Jensen, D., Fagherazzi, S., 2023a. Quantifying flow velocities in river deltas via remotely sensed suspended sediment concentration. Geophys. Res. Lett. 50 (4), e2022GL101392.

Donatelli, C., Cortese, L., Fagherazzi, S., 2023b. Delta-X: Delft3D Sediment Model, Site 421, Terrebonne Basin, MRD, Louisiana, USA. ORNL DAAC, Oak Ridge, Tennessee, USA. https://doi.org/10.3334/ORNLDAAC/2304.

Donatelli, C., Passalacqua, P., Jensen, D., Oliver-Cabrera, T., Jones, C.E., Fagherazzi, S., 2023c. Spatial variability in salt marsh drainage controlled by small scale topography. J. Geophys. Res.: Earth Surf. 128 (11), e2023JF007219.

Dronova, I., Taddeo, S., Hemes, K.S., Knox, S.H., Valach, A., Oikawa, P.Y., Baldocchi, D. D., 2021. Remotely sensed phenological heterogeneity of restored wetlands: linking vegetation structure and function. Agric. For. Meteorol. 296, 108215.

Edmonds, D.A., Toby, S.C., Siverd, C.G., Twilley, R., Bentley, S.J., Hagen, S., Xu, K., 2023. Land loss due to human-altered sediment budget in the Mississippi River Delta. Nat. Sustainability 6 (6), 644–651.

Fagherazzi, S., Kirwan, M.L., Mudd, S.M., Guntenspergen, G.R., Temmerman, S., D'Alpaos, A., Clough, J., 2012. Numerical models of salt marsh evolution: ecological, geomorphic, and climatic factors. Rev. Geophys. 50 (1), RG1002.

Fagherazzi, S., Mariotti, G., Leonardi, N., Canestrelli, A., Nardin, W., Kearney, W.S., 2020. Salt marsh dynamics in a period of accelerated sea level rise. J. Geophys. Res.: Earth Surf. 125 (8), e2019JF005200.

Fichot, C.G., Harringmeyer, J., 2022. Delta-X: in situ beam attenuation and particle size from LISST-200X, 2021. ORNL DAAC, Oak Ridge, Tennessee, USA. https://doi.org/10.3334/ORNLDAAC/2077.

Fichot, C.G., Harringmeyer, J., 2023a. Delta-X: AVIRIS-NG L3-derived water quality, TSS, and turbidity, MRD, V3. ORNL DAAC, Oak Ridge, Tennessee, USA. https://doi.org/10.3334/ORNLDAAC/2152.
Fichot, C.G., Harringmeyer, J., 2023b. Delta-X: in situ water surface reflectance across MRD, LA, USA, 2021, V3. ORNL DAAC, Oak Ridge, TN, USA. https://doi.org/10.3334/ORNLDAAC/2076.
Fichot, C.G., Ghosh, N., Harringmeyer, J., Weiser, M., 2022a. Delta-X: Total suspended solids concentration across MRD, LA, USA, 2021, version 2. ORNL DAAC, Oak Ridge, Tennessee, USA. https://doi.org/10.3334/ORNLDAAC/2075.
Fichot, C.G., Ghosh, N., Harringmeyer, J., Weiser, M., 2022b. Delta-X: particulate organic carbon concentration from water samples, MRD, LA, 2021. ORNL DAAC, Oak Ridge, Tennessee, USA. https://doi.org/10.3334/ORNLDAAC/2073.
Fichot, C.G., Harringmeyer, J., Weiser, M., 2022c. Delta-X: In Situ Water Quality Indicators across MRD, LA, USA, 2021c, Version 2. ORNL DAAC, Oak Ridge, Tennessee, USA. https://doi.org/10.3334/ORNLDAAC/2080.
Fitzpatrick, C., Jankowski, K.L., Reed, D., 2021. 2023 Coastal Master Plan: Attachment B3: Determining Subsidence Rates for Use in Predictive Modeling, Version 3. Coastal Protection and Restoration Authority, Baton Rouge, Louisiana, USA. https://coastal.la.gov/wp-content/uploads/2023/08/B3_DeterminingSubsidenceRates_Mar2021_v3.pdf.
Folse, T.M., McGinnis, T.E., Sharp, L.A., West, J.L., Hymel, M.K., Troutman, J.P., Beck, H. J., 2020. A Standard Operating Procedures Manual for the Coastwide Reference Monitoring System-Wetlands and the System-Wide Assessment and Monitoring Program: Methods for Site Establishment, Data Collection, and Quality Assurance/Quality Control. Louisiana Coastal Protection and Restoration Authority, Baton Rouge, LA. https://cims.coastal.louisiana.gov/RecordDetail.aspx?Root=0&sid=24216.
Fontenot, A., 2022. Wetland Soil Development along Salinity and Hydrogeomorphic Gradients in Active and Inactive Deltaic Basins of Coastal Louisiana. LSU Master's thesis,. Louisiana State University, p. 5622. https://repository.lsu.edu/gradschool_theses/5622/.
Fore, A.G., Chapman, B.D., Hawkins, B.P., Hensley, S., Jones, C.E., Michel, T.R., Muellerschoen, R.J., 2015. UAVSAR polarimetric calibration. IEEE Trans. Geosci. Remote Sens. 53 (6), 3481–3491.
French, J.R., 1993. Numerical simulation of vertical marsh growth and adjustment to accelerated sea-level rise, North Norfolk, UK. Earth Surf. Process. Landf. 18 (1), 63–81.
Galloway, W.E., 1975. Process Framework for Describing the Morphologic and Stratigraphic Evolution of Deltaic Depositional Systems. Models of Exploration, American Association of Petroleum Geologists, Deltas, pp. 87–98.
Ganti, V., Lamb, M.P., McElroy, B., 2014. Quantitative bounds on morphodynamics and implications for reading the sedimentary record. Nat. Commun. 5 (1), 3298.
Gelfenbaum, G., Stevens, A.W., Miller, I., Warrick, J.A., Ogston, A.S., Eidam, E., 2015. Large-scale dam removal on the Elwha River, Washington, USA: coastal geomorphic change. Geomorphology 246, 649–668.
Gesch, D., Oimoen, M., Greenlee, S., Nelson, C., Steuck, M., Tyler, D., 2002. The national elevation dataset. Photogramm. Eng. Remote. Sens. 68 (1), 5–32.
Giosan, L., Syvitski, J., Constantinescu, S., Day, J., 2014. Climate change: protect the world's deltas. Nature 516 (7529), 31–33.
Glick, P., Clough, J., Polaczyk, A., Couvillion, B., Nunley, B., 2013. Potential effects of sea-level rise on coastal wetlands in southeastern Louisiana. J. Coast. Res. 63, 211–233.
Greenberg, E., Thompson, D.R., Jensen, D., Townsend, P.A., Queally, N., Chlus, A., Simard, M., 2022. An improved scheme for correcting remote spectral surface reflectance simultaneously for terrestrial BRDF and water-surface sunglint in coastal environments. J. Geophys. Res. Biogeosci. 127 (3), e2021JG006712.
Harringmeyer, J.P., Ghosh, N., Weiser, M.W., Thompson, D.R., Simard, M., Lohrenz, S.E., Fichot, C.G., 2024. A hyperspectral view of the nearshore Mississippi River Delta: characterizing suspended particles in coastal wetlands using imaging spectroscopy. Remote Sens. Environ. 301, 113943.
Hauer, M.E., Fussell, E., Mueller, V., Burkett, M., Call, M., Abel, K., Wrathall, D., 2020. Sea-level rise and human migration. Nat. Rev. Earth Environ. 1 (1), 28–39.
Hiatt, M., Passalacqua, P., 2015. Hydrological connectivity in river deltas: the first-order importance of channel-island exchange. Water Resour. Res. 51 (4), 2264–2282.
Hiatt, M., Passalacqua, P., 2017. What controls the transition from confined to unconfined flow? Analysis of hydraulics in a coastal river delta. J. Hydraul. Eng. 143 (6), 03117003.
Hiatt, M., Castañeda-Moya, E., Twilley, R., Hodges, B.R., Passalacqua, P., 2018. Channel-island connectivity affects water exposure time distributions in a coastal river delta. Water Resour. Res. 54 (3), 2212–2232.
Jalonen, J., Järvelä, J., Virtanen, J.P., Vaaja, M., Kurkela, M., Hyyppä, H., 2015. Determining characteristic vegetation areas by terrestrial laser scanning for floodplain flow modeling. Water 7 (2), 420–437.
Jensen, D.J., Simard, M., Cavanaugh, K.C., Thompson, D.R., 2017. Imaging spectroscopy BRDF correction for mapping Louisiana's coastal ecosystems. IEEE Trans. Geosci. Remote Sens. 56 (3), 1739–1748.
Jensen, D., Cavanaugh, K.C., Simard, M., Okin, G.S., Castañeda-Moya, E., McCall, A., Twilley, R.R., 2019a. Integrating imaging spectrometer and synthetic aperture radar data for estimating wetland vegetation aboveground biomass in coastal Louisiana. Remote Sens. 11 (21), 2533.
Jensen, D., Simard, M., Cavanaugh, K., Sheng, Y., Fichot, C.G., Pavelsky, T., Twilley, R., 2019b. Improving the transferability of suspended solid estimation in wetland and deltaic waters with an empirical hyperspectral approach. Remote Sens. 11 (13), 1629.
Jensen, D.J., Cavanaugh, K.C., Thompson, D.R., Fagherazzi, S., Cortese, L., Simard, M., 2022. Leveraging the historical Landsat catalog for a remote sensing model of wetland accretion in coastal Louisiana. J. Geophys. Res. Biogeosci. 127 (6), e2022JG006794.
Jensen, D.J., Castañeda-Moya, E., Solohin, E., Thompson, D.R., Simard, M., 2024a. Delta-X AVIRIS-NG L3 Derived Vegetation Types. ORNL DAAC, Oak Ridge, Tennessee, USA, MRD, Louisiana, USA. https://doi.org/10.3334/ORNLDAAC/2457. V2 (Version 2).
Jensen, D., Thompson, D.R., Simard, M., Solohin, E., Castañeda-Moya, E., 2024b. Imaging spectroscopy-based estimation of aboveground biomass in Louisiana's coastal wetlands: toward consistent spectroscopic retrievals across atmospheric states. J. Geophys. Res. Biogeosci. 129 (9). https://doi.org/10.1029/2024JG008112.
Jensen, D.J., Castañeda-Moya, E., Solohin, E., Thompson, D.R., Simard, M., 2025a. Delta-X: AVIRIS-NG L3 Derived Herbaceous Aboveground Biomass, MRD, Louisiana, USA, V3 (Version 3). ORNL Distributed Active Archive Center. https://doi.org/10.3334/ORNLDAAC/2409.
Jensen, D.J., Castañeda-Moya, E., Solohin, E., Denbina, M., Thompson, D.R., Simard, M., 2025b. AVIRIS-NG and UAVSAR L3 derived Forest aboveground biomass, MRD, LA, USA, 2021. ORNL DAAC, Oak Ridge, Tennessee, USA. https://doi.org/10.3334/ORNLDAAC/2410.
Jensen, D.J., Solohin, E., Castañeda-Moya, E., Thompson, D.R., Simard, M., 2025c. Delta-X AVIRIS-NG L2B derived fractional cover, MRD, LA, USA, 2021. ORNL DAAC, Oak Ridge, Tennessee, USA. https://doi.org/10.3334/ORNLDAAC/2407.
Jensen, D.J., Castañeda-Moya, E., Solohin, E., Simard, M., 2025d. Delta-X: AVIRIS-NG L3 Derived Herbaceous Belowground Biomass, MRD, Louisiana, USA, 2021. ORNL DAAC, Oak Ridge, Tennessee, USA. https://doi.org/10.3334/ORNLDAAC/2456.
Jevrejeva, S., Jackson, L.P., Riva, R.E., Grinsted, A., Moore, J.C., 2016. Coastal sea level rise with warming above 2 C. Proc. Natl. Acad. Sci. 113 (47), 13342–13347.
Jiang, D., Matsushita, B., Pahlevan, N., Gurlin, D., Lehmann, M.K., Fichot, C.G., O'Donnell, D., 2021. Remotely estimating total suspended solids concentration in clear to extremely turbid waters using a novel semi-analytical method. Remote Sens. Environ. 258, 112386.
Jones, C., Simard, M., Lou, Y., 2021. Pre-Delta-X: UAVSAR-derived water level change maps, Atchafalaya Basin, LA, USA, 2016. ORNL DAAC, Oak Ridge, Tennessee, USA. https://doi.org/10.3334/ORNLDAAC/1823.
Jones, C., Oliver-Cabrera, T., Simard, M., Lou, Y., 2022a. Delta-X: UAVSAR L3 water level changes, MRD, Louisiana, 2021. ORNL DAAC, Oak Ridge, Tennessee, USA. https://doi.org/10.3334/ORNLDAAC/2058.
Jones, C., Oliver-Cabrera, T., Simard, M., Lou, Y., 2022b. Delta-X: UAVSAR L2 interferometric products, MRD, Louisiana, 2021. ORNL DAAC, Oak Ridge, Tennessee, USA. https://doi.org/10.3334/ORNLDAAC/2057.
Jones, C., Oliver-Cabrera, T., Simard, M., Lou, Y., 2022c. Delta-X: UAVSAR L1B interferometric products, MRD, Louisiana, 2021. ORNL DAAC, Oak Ridge, Tennessee, USA. https://doi.org/10.3334/ORNLDAAC/1979.
Jones, C., Simard, M., Lou, Y., Oliver-Cabrera, T., 2022d. Delta-X: UAVSAR L1 single look complex (SLC) stack products, MRD, Louisiana, 2021. ORNL DAAC, Oak Ridge, Tennessee, USA. https://doi.org/10.3334/ORNLDAAC/1984.
Jones, C., Varugu, B., Oliver-Cabrera, T., Simard, M., Lou, Y., 2024. Delta-X: UAVSAR L3 Gridded Open Water Channels, MRD, LA, USA, 2021, V2. ORNL DAAC, Oak Ridge, Tennessee, USA. https://doi.org/10.3334/ORNLDAAC/2344.
Karegar, M.A., Dixon, T.H., Malservisi, R., Kusche, J., Engelhart, S.E., 2017. Nuisance flooding and relative sea-level rise: the importance of present-day land motion. Sci. Rep. 7 (1), 1–9.
Keogh, M.E., Törnqvist, T.E., 2019. Measuring rates of present-day relative sea-level rise in low-elevation coastal zones: a critical evaluation. Ocean Sci. 15 (1), 61–73.
Keogh, M.E., Törnqvist, T.E., Kolker, A.S., Erkens, G., Bridgeman, J.G., 2021. Organic matter accretion, shallow subsidence, and river delta sustainability. J. Geophys. Res.: Earth Surf. 126 (12), e2021JF006231.
Khojasteh, D., Glamore, W., Heimhuber, V., Felder, S., 2021. Sea level rise impacts on estuarine dynamics: a review. Sci. Total Environ. 780, 146470.
Kroes, D.E., 2022. Mean Bed Elevations of Waterbodies on the Atchafalaya River Floodplain. U.S. Geological Survey data release. https://doi.org/10.5066/P94GULXE.
Kulp, S.A., Strauss, B.H., 2019. New elevation data triple estimates of global vulnerability to sea-level rise and coastal flooding. Nat. Commun. 10 (1), 1–12.
Leonard, L., Reed, D.J., 2002. Hydrodynamics and sediment transport through tidal marsh canopies. J. Coast. Res. 36, 459–469.
Liao, T.H., Simard, M., Denbina, M., Lamb, M.P., 2020. Monitoring water level change and seasonal vegetation change in the coastal wetlands of Louisiana using L-band time-series. Remote Sens. 12 (15), 2351.
Liu, D., Wang, X., Aminjafari, S., Yang, W., Cui, B., Yan, S., Jaramillo, F., 2020. Using InSAR to identify hydrological connectivity and barriers in a highly fragmented wetland. Hydrol. Process. 34 (23), 4417–4430.
Long, C.M., Pavelsky, T.M., 2013. Remote sensing of suspended sediment concentration and hydrologic connectivity in a complex wetland environment. Remote Sens. Environ. 129, 197–209.
Love, M., Amante, C., Taylor, L.A., Carignan, K.S., 2012. Digital elevation models of the northern Gulf Coast: Procedures, data sources and analysis. In: NOAA Technical Memorandum NESDIS NGDG-59. National Geophysical Data Center, Marine Geology and Geophysics Division. National Oceanic and Atmospheric Administration, Boulder, Colorado. https://ntrl.ntis.gov/NTRL/ (accession number PB2012108808, NTIS Issue 201226).
Lu, Z., Kwoun, O.I., 2008. Radarsat-1 and ERS InSAR analysis over southeastern coastal Louisiana: implications for mapping water-level changes beneath swamp forests. IEEE Trans. Geosci. Remote Sens. 46 (8), 2167–2184.
Mariotti, G., Huang, H., Xue, Z., Li, B., Justic, D., Zang, Z., 2018. Biased wind measurements in estuarine waters. J. Geophys. Res. Oceans 123 (5), 3577–3587.

Marlier, M.E., Resetar, S.A., Lachman, B.E., Anania, K., Adams, K., 2022. Remote sensing for natural disaster recovery: lessons learned from hurricanes Irma and Maria in Puerto Rico. Environ. Sci. Pol. 132, 153–159.
Masselink, G., Hughes, M., Knight, J., 2014. Introduction to Coastal Processes and Geomorphology. Routledge.
Morris, J.T., Bowden, W.B., 1986. A mechanistic, numerical model of sedimentation, mineralization, and decomposition for marsh sediments. Soil Sci. Soc. Am. J. 50 (1), 96–105.
Morris, J.T., Barber, D.C., Callaway, J.C., Chambers, R., Hagen, S.C., Hopkinson, C.S., Wigand, C., 2016. Contributions of organic and inorganic matter to sediment volume and accretion in tidal wetlands at steady state. Earth's Future 4 (4), 110–121.
Mudd, S.M., Howell, S.M., Morris, J.T., 2009. Impact of dynamic feedbacks between sedimentation, sea-level rise, and biomass production on near-surface marsh stratigraphy and carbon accumulation. Estuar. Coast. Shelf Sci. 82 (3), 377–389.
Nardin, W., Edmonds, D.A., 2014. Optimum vegetation height and density for inorganic sedimentation in deltaic marshes. Nat. Geosci. 7 (10), 722–726.
Nechad, B., Ruddick, K.G., Park, Y., 2010. Calibration and validation of a generic multisensor algorithm for mapping of total suspended matter in turbid waters. Remote Sens. Environ. 114 (4), 854–866.
Neumann, B., Vafeidis, A.T., Zimmermann, J., Nicholls, R.J., 2015. Future coastal population growth and exposure to sea-level rise and coastal flooding - a global assessment. PLoS One 10 (3), e0118571.
Nghiem, J., 2022. Sediment Accretion Rates and Spatial Patterns in the Wax Lake Delta, LA 2020. National Center for Airborne Laser Mapping (NCALM). Distributed by OpenTopography. https://doi.org/10.5069/G99W0CP6.
Nghiem, J., Salter, G., Wright, K.A., Passalacqua, P., Lamb, M.P., 2022. Delta-X: turbidity, water and air pressure, temperature, MRD, Louisiana, 2021, V4. ORNL DAAC, Oak Ridge, Tennessee, USA. https://doi.org/10.3334/ORNLDAAC/2241.
Nghiem, J., Salter, G., Lamb, M.P., 2023. Delta-X: Bed and Suspended Sediment Grain Size, MRD, LA, USA, 2021, Version 2. ORNL DAAC, Oak Ridge, Tennessee, USA. https://doi.org/10.3334/ORNLDAAC/2135.
Nghiem, J.A., Li, G.K., Harringmeyer, J.P., Salter, G., Fichot, C.G., Cortese, L., Lamb, M. P., 2024. Testing floc settling velocity models in rivers and freshwater wetlands. Earth Surf. Dyn. 12 (6), 1267–1294.
Nicholls, R.J., Lincke, D., Hinkel, J., Brown, S., Vafeidis, A.T., Meyssignac, B., Fang, J., 2021. A global analysis of subsidence, relative sea-level change and coastal flood exposure. Nat. Clim. Chang. 11 (4), 338–342.
Nienhuis, J.H., Kim, W., Milne, G.A., Quock, M., Slangen, A.B., Törnqvist, T.E., 2023. River deltas and sea-level rise. Annu. Rev. Earth Planet. Sci. 51 (1), 79–104.
Ohenhen, L.O., Shirzaei, M., Ojha, C., Kirwan, M.L., 2023. Hidden vulnerability of US Atlantic coast to sea-level rise due to vertical land motion. Nat. Commun. 14 (1), 2038.
Oliver-Cabrera, T., Wdowinski, S., 2016. InSAR-based mapping of tidal inundation extent and amplitude in Louisiana coastal wetlands. Remote Sens. 8 (5), 393.
Oliver-Cabrera, T., Jones, C.E., Yunjun, Z., Simard, M., 2021. InSAR phase unwrapping error correction for rapid repeat measurements of water level change in wetlands. IEEE Trans. Geosci. Remote Sens. 60, 1–15.
Oliver-Cabrera, T., Jones, C.E., Simard, M., Varugu, B., Belhadj-Aissa, S., 2025. Identifying wet troposphere delay in L-band InSAR using weather radar reflectivity. Earth and Space Science 12, e2025EA004382.
Paola, C., Voller, V.R., 2005. A generalized Exner equation for sediment mass balance. J. Geophys. Res.: Earth Surf. 110, F04014.
Paola, C., Twilley, R.R., Edmonds, D.A., Kim, W., Mohrig, D., Parker, G., Voller, V.R., 2011. Natural processes in delta restoration: application to the Mississippi Delta. Annu. Rev. Mar. Sci. 3 (1), 67–91.
Passeri, D.L., Hagen, S.C., Medeiros, S.C., Bilskie, M.V., Alizad, K., Wang, D., 2015. The dynamic effects of sea level rise on low-gradient coastal landscapes: a review. Earth's Future 3 (6), 159–181.
Payandeh, A.R., Justic, D., Mariotti, G., Huang, H., Sorourian, S., 2019. Subtidal water level and current variability in a bar-built estuary during cold front season: Barataria Bay, Gulf of Mexico. J. Geophys. Res.Oceans 124 (10), 7226–7246.
Payandeh, A.R., Simard, M., 2025a. Delta-X: Delft3D FM, Extended Domain Hydrodynamic Model. ORNL DAAC. Oak Ridge, Tennessee, USA. https://doi.org/10.3334/ORNLDAAC/2464.
Payandeh, A.R., M. Simard, and C. Jones. 2025b. Delta-X: Delft3D FM, Weighted Mean Hydroperiod, MRD, Louisiana, USA. ORNL DAAC, Oak Ridge, Tennessee, USA. https://doi.org/10.3334/ORNLDAAC/2421.
Payandeh, A.R., M. Simard, and C. Jones. 2025c. Delta-X: Delft3D FM, Weighted Mean Salinity, MRD, Louisiana, USA. ORNL DAAC, Oak Ridge, Tennessee, USA. https://doi.org/10.3334/ORNLDAAC/2420.
Perez, B.C., Day Jr., J.W., Rouse, L.J., Shaw, R.F., Wang, M., 2000. Influence of Atchafalaya River discharge and winter frontal passage on suspended sediment concentration and flux in Fourleague Bay, Louisiana. Estuar. Coast. Shelf Sci. 50 (2), 271–290. https://doi.org/10.1006/ecss.1999.0564.
Rangoonwala, A., Jones, C.E., Ramsey III, E., 2016. Wetland shoreline recession in the Mississippi River Delta from petroleum oiling and cyclonic storms. Geophys. Res. Lett. 43 (22), 11–652.
Restreppo, G.A., Bentley, S.J., Wang, J., Xu, K., 2019. Riverine sediment contribution to distal deltaic wetlands: Fourleague Bay, LA. Estuar. Coasts 42, 55–67. https://doi.org/10.1007/s12237-018-0453-0.
Ritchie, J.C., McHenry, J.R., 1990. Application of radioactive fallout cesium-137 for measuring soil erosion and sediment accumulation rates and patterns: a review. J. Environ. Qual. 19 (2), 215–233.
Roberts, H.H., 1997. Dynamic changes of the Holocene Mississippi River delta plain: the delta cycle. J. Coast. Res. 13 (3), 605–627.
Roberts, S., Nielsen, O., Gray, D., Sexton, J., & Davies, G. (2015). ANUGA user manual, Release 2.0. doi:10.13140/RG.2.2.12401.99686.
Rovai, A.S., Twilley, R.R., Christensen, A., McCall, A., Jensen, D.J., Snedden, G.A., Morris, J.T., Cavell, J.A., 2022. Biomass allocation of tidal freshwater marsh species in response to natural and manipulated hydroperiod in coastal deltaic floodplains. Estuar. Coast. Shelf Sci. 268, 107784.
Roy, S., Robeson, S.M., Ortiz, A.C., Edmonds, D.A., 2020. Spatial and temporal patterns of land loss in the lower Mississippi River Delta from 1983 to 2016. Remote Sens. Environ. 250, 112046.
Salter, G., Lamb, M.P., 2022. Autocyclic secondary channels stabilize deltaic islands undergoing relative sea level rise. Geophys. Res. Lett. 49, e2022GL098885. https://doi.org/10.1029/2022GL098885.
Salter, G., Passalacqua, P., Wright, K., Feil, S., Jensen, D., Simard, M., Lamb, M.P., 2022. Spatial patterns of deltaic deposition revealed by streaklines extracted from remotely-sensed suspended sediment concentration. Geophys. Res. Lett. 49, e2022GL098443. https://doi.org/10.1029/2022GL098443.
Shahzad, M.I., Meraj, M., Nazeer, M., Zia, I., Inam, A., Mehmood, K., Zafar, H., 2018. Empirical estimation of suspended solids concentration in the Indus Delta region using Landsat-7 ETM+ imagery. J. Environ. Manag. 209, 254–261.
Shribman, Z.I., 2021. Blue carbon in South Florida's mangroves: the role of large roots and Necromass. LSU Master's Theses. 5433. https://repository.lsu.edu/gradschool_theses/5433.
Simard, M., Denbina, M.W., Rodriguez, E., Christensen, A.L., Wright, K.A., Rovai, A., 2022. Delta-X: cell products across the MRD, LA, USA, 2021. ORNL DAAC, Oak Ridge, Tennessee, USA. https://doi.org/10.3334/ORNLDAAC/2108.
Sorourian, S., Huang, H., Li, C., Justic, D., Payandeh, A.R., 2020. Wave dynamics near Barataria Bay tidal inlets during spring–summer time. Ocean Modelling 147, 101553.
Sullivan, J.C., Torres, R., Garrett, A., Blanton, J., Alexander, C., Robinson, M., Hayes, D., 2015. Complexity in salt marsh circulation for a semienclosed basin. J. Geophys. Res.: Earth Surf. 120 (10), 1973–1989.
Syvitski, J.P., Kettner, A.J., Overeem, I., Hutton, E.W., Hannon, M.T., Brakenridge, G.R., Nicholls, R.J., 2009. Sinking deltas due to human activities. Nat. Geosci. 2 (10), 681–686.
Syvitski, J., Anthony, E., Saito, Y., Zăinescu, F., Day, J., Bhattacharya, J.P., Giosan, L., 2022. Large deltas, small deltas: toward a more rigorous understanding of coastal marine deltas. Glob. Planet. Chang. 218, 103958.
Tang, W., Zhan, W., Jin, B., Motagh, M., Xu, Y., 2021. Spatial variability of relative sea-level rise in Tianjin, China: insight from InSAR, GPS, and tide-gauge observations. IEEE J. Select. Topi. Appl. Earth Observat. Remote Sensing 14, 2621–2633.
Temmerman, S., Kirwan, M.L., 2015. Building land with a rising sea. Science 349 (6248), 588–589.
Thompson, D.R., Jensen, D.J., Chapman, J.W., Simard, M., Greenberg, E.. Delta-X: AVIRIS-NG BRDF-Adjusted Surface Reflectance and Mosaics, MRD, LA 2021, V3 (Version 3). ORNL Distributed Active Center. https://doi.org/10.3334/ORNLDAAC/2355.
Thompson, D.R., Natraj, V., Green, R.O., Helmlinger, M.C., Gao, B.C., Eastwood, M.L., 2018. Optimal estimation for imaging spectrometer atmospheric correction. Remote Sens. Environ. 216, 355–373. https://doi.org/10.1016/j.rse.2018.07.003.
Thompson, D.R., Cawse-Nicholson, K., Erickson, Z., Fichot, C.G., Frankenberg, C., Gao, B. C., Thompson, A., 2019. A unified approach to estimate land and water reflectances with uncertainties for coastal imaging spectroscopy. Remote Sens. Environ. 231, 111198. https://doi.org/10.1016/j.rse.2019.05.017.
Thompson, D.R., Jensen, D.J., Chapman, J., Greenberg, E., Simard, M., 2022a. Delta-X: AVIRIS-NG L1B spectral radiance products, MRD, Louisiana, 2021. ORNL DAAC, Oak Ridge, Tennessee, USA. https://doi.org/10.3334/ORNLDAAC/1987.
Thompson, D.R., Jensen, D.J., Chapman, J.W., Greenberg, E., Simard, M., 2022b. Delta-X: AVIRIS-NG L2 Surface Reflectance, MRD Louisiana, 2021. ORNL DAAC, Oak Ridge, Tennessee, USA. https://doi.org/10.3334/ORNLDAAC/1988.
Twilley, R.R., Day, J.W., Bevington, A.E., Castañeda-Moya, E., Christensen, A., Holm, G., Heffner, L.R., Lane, R.R., McCall, A., Aarons, A., Li, S., Rovai, A.S., 2019a. Ecogeomorphology of coastal deltaic floodplains and estuaries in an active delta: insights from the Atchafalaya Coastal Basin. Estuarine, Coastal. Shelf Science 106341.
Twilley, R.R., Day, J.W., Bevington, A.E., Castañeda-Moya, E., Christensen, A., Holm, G., Rovai, A.S., 2019b. Ecogeomorphology of coastal deltaic floodplains and estuaries in an active delta: insights from the Atchafalaya Coastal Basin. Estuar. Coast. Shelf Sci. 227, 106341. https://doi.org/10.1016/j.ecss.2019.106341.
Twilley, R., Biswas, P., Rovai, A., Cassaway, A.F., Christensen, A.L., Vargas-Lopez, I.A., Kameshwar, S., 2024a. Delta-X: Cesium-137 soil accretion rates and NUMAR validation, MRD, 2021. ORNL DAAC, Oak Ridge, Tennessee, USA. https://doi.org/10.3334/ORNLDAAC/2380.
Twilley, R., Cassaway, A.F., Rovai, A., Vargas-Lopez, I.A., Pineda-gomez, J.A., 2024b. Delta-X: feldspar sediment accretion measurements, MRD, LA, USA, 2019-2023, version 4. ORNL DAAC, Oak Ridge, Tennessee, USA. https://doi.org/10.3334/ORNLDAAC/2381.
Twilley, R., Biswas, P., Rovai, A., Christensen, A.L., Cassaway, A.F., Vargas-Lopez, I.A., 2024c. Delta-X: NUMAR Soil Accretion Modeled to 2100, MRD, Louisiana, USA. ORNL DAAC, Oak Ridge, Tennessee, USA. https://doi.org/10.3334/ORNLDAAC/2368.
Twilley, R., Biswas, P., Rovai, A., Christensen, A.L., Cassaway, A.F., Vargas-Lopez, I.A., Kameshwar, S., 2024d. Delta-X: NUMAR predictive model for marsh accretion rates and chemical properties. ORNL DAAC, Oak Ridge, Tennessee, USA. https://doi.org/10.3334/ORNLDAAC/2354.
Valentine, K., Mariotti, G., 2019. Wind-driven water level fluctuations drive marsh edge erosion variability in microtidal coastal bays. Cont. Shelf Res. 176, 76–89.

Varugu, B.K., Jones, C.E., Oliver-Cabrera, T., Simard, M., Jensen, D.J., 2025. Study of hydrologic connectivity and tidal influence on water flow within Louisiana coastal wetlands using rapid-repeat interferometric synthetic aperture radar. Remote Sens. 17 (3), 459. https://doi.org/10.3390/rs17030459.

Vasilopoulos, G., Quan, Q.L., Parsons, D.R., Darby, S.E., Tri, V.P.D., Hung, N.N., Aalto, R., 2021. Establishing sustainable sediment budgets is critical for climate-resilient mega-deltas. Environ. Res. Lett. 16 (6), 064089.

Walling, D.E., He, Q., 1997. Use of fallout ^{137}Cs in investigations of overbank sediment deposition on river floodplains. Catena 29 (3–4), 263–282.

Wang, J., Xu, K., Restreppo, G.A., Bentley, S.J., Meng, X., Zhang, X., 2018. The coupling of bay hydrodynamics to sediment transport and its implication in micro-tidal wetland sustainability. Mar. Geol. 405, 68–76. https://doi.org/10.1016/j.margeo.2018.08.005.

Wang, D., Salter, G., Lamb, M.P., 2023. Delta-X: Matlab model for wax Lake Delta land accretion. ORNL DAAC, Oak Ridge, Tennessee, USA. https://doi.org/10.3334/ORNLDAAC/2309.

Wang, K., Chen, J., Valseth, E., Wells, G., Bettadpur, S., Jones, C.E., Dawson, C., 2024. Subtle land subsidence elevates future storm surge risks along the Gulf coast of the United States. J. Geophys. Res.: Earth Surf. 129 (9), e2024JF007858.

Water Institute of the Gulf (Water Institute), 2019. Monitoring Plans for Louisiana's System-Wide Assessment and Monitoring Program (SWAMP), Version IV. Prepared for and Funded by the Coastal Protection and Restoration Authority (CPRA) under Task Order 6, Contract no. 2503-12-58. Baton Rouge, LA, p. 235.

Wdowinski, S., Amelung, F., Miralles-Wilhelm, F., Dixon, T.H., Carande, R., 2004. Space-based measurements of sheet-flow characteristics in the Everglades wetland, Florida. Geophys. Res. Lett. 31 (15).

Wellner, R., Beaubouef, R., Van Wagoner, J., Roberts, H.H., Sun, T., Wagoner, J.V., 2005. Jet-plume depositional bodies; the primary building blocks of wax Lake Delta. Trans. Gulf Coast Assoc. Geol. Soc. 55, 867–909.

Wright, K., Hiatt, M., Passalacqua, P., 2018. Hydrological connectivity in vegetated river deltas: the importance of patchiness below a threshold. Geophys. Res. Lett. 45 (19), 10–416.

Wright, K., Passalacqua, P., Simard, M., Jones, C.E., 2022. Integrating connectivity into hydrodynamic models: an automated open-source method to refine an unstructured mesh using remote sensing. J. Adv. Model. Earth Syst. 14 (8), e2022MS003025. https://doi.org/10.1029/2022MS003025.

Wu, P.C., Wei, M., D'Hondt, S., 2022. Subsidence in coastal cities throughout the world observed by InSAR. Geophys. Res. Lett. 49 (7), e2022GL098477.

Xing, F., Syvitski, J.P., Kettner, A.J., Meselhe, E.A., Atkinson, J.H., Khadka, A.K., 2017. Morphological responses of the wax Lake Delta, Louisiana, to hurricanes Rita. Elem Sci Anth 5, 80.

Zhang, X., Jones, C.E., Oliver-Cabrera, T., Simard, M., Fagherazzi, S., 2022a. Using rapid repeat SAR interferometry to improve hydrodynamic models of flood propagation in coastal wetlands. Adv. Water Resour. 159, 104088.

Zhang, X., Wright, K., Passalacqua, P., Simard, M., Fagherazzi, S., 2022b. Improving channel hydrological connectivity in coastal hydrodynamic models with remotely sensed channel networks. J. Geophys. Res.: Earth Surf. 127 (3), e2021JF006294.

Zhang, X., Jones, C.E., Simard, M., Passalacqua, P., Oliver-Cabrera, T., Fagherazzi, S., 2024. Vegetation promotes flow retardation and retention in deltaic wetlands. Limnology and Oceanography Letters 9, 644–652. https://doi.org/10.1002/lol2.10376.

Zundel, A.K., 2000. Surface-Water Modeling System Reference Manual. Brigham Young University, Environmental Modeling Research Laboratory, Provo, UT, p. 79.